



# **PISCES**

## **A Morphodynamic Coastal Area Model Final Report**

**D M Price  
T J Cheshier  
H N Southgate**

**Report SR 411  
April 1995**



**Address and Registered Office: HR Wallingford Ltd, Howbery Park, Wallingford, Oxon OX10 8BA  
Tel: + 44 (0)1491 835361 Fax: + 44 (0)1491 832233**

**Registered in England No. 2562069. HR Wallingford is a wholly owned subsidiary of HR Wallingford Group Ltd.**





---

## Contract

---

This report describes work funded by the Ministry of Agriculture, Fisheries and Food under Contract Number CSA 2090, for which the nominated officer was Mr B D Richardson and the HR Wallingford (HR) nominated officer was Dr W R White. Allied work funded by the Commission of the European Communities Directorate General for Science, Research and Development under Contract Number MAS2-CT92-0027 is reported here as well. The HR job number was IDS 11. This report is published on behalf of the Ministry of Agriculture, Fisheries and Food, but any opinions expressed in this report are not necessarily those of the funding Ministry. The work was carried out by D M Price and T J Cheshier and the project was managed by Dr H N Southgate.

Prepared by

D.M. Price  
(name)

MATHEMATICAL MODELLER  
(Job title)

Approved by

H.N. Southgate

PROJECT MANAGER

Date

20-4-95

© HR Wallingford Limited 1995





---

## **Summary**

---

### **PISCES**

#### **A Morphodynamic Coastal Area Model Final Report**

**D M Price  
T J Chesher  
H N Southgate**

**Report SR 411  
January 1995**

This report describes work carried out during a three year research study funded by MAFF, to develop an integrated morphodynamic coastal area numerical model. The model is designed primarily to investigate the response of a particular coastal system to short term events (up to a spring-neap cycle) by simulating the relevant hydrodynamics, sediment transport and resulting seabed level changes.

The first year of the study was spent integrating wave, current, sediment transport and morphodynamic models into one model, called PISCES. Application and testing was carried out on a number of idealised test cases, and a complete description of this work is reported in HR report SR337.

In years two and three further development has been carried out on PISCES, along with the application of the model to more test cases, both idealised and real. These applications have produced realistic results, and have also highlighted areas within the model which may need to be developed further.

This report is unrestricted and contains the outcome of original research. It is intended primarily for numerical modellers in civil engineering hydraulics. For further information regarding this study please contact Dr H N Southgate in the Marine Sediments Group.





---

## List of symbols

---

|             |  |
|-------------|--|
| $D$         | non-dimensional grain diameter                     |
| $D_w$       | mean rate of wave energy dissipation per unit area |
| $D$         | diffusion coefficient                              |
| $d$         | water depth  |
| $g$         | gravitational acceleration                         |
| $H_{rms}$   | root mean square wave height                       |
| $H_s$       | significant wave height                            |
| $h$         | seabed level relative to model datum               |
| $T_p$       | peak wave period                                   |
| $U$         | friction velocity                                  |
| $u$         | current velocity in x direction                    |
| $v$         | current velocity in y direction                    |
| $z$         | free surface elevation relative to model datum     |
| $\nu$       | eddy viscosity                                     |
| $\rho$      | density of water                                   |
| $\tau_{bx}$ | bed shear stress in x direction                    |
| $\tau_{by}$ | bed shear stress in y direction                    |
| $\tau_{wx}$ | wave breaking stress in x direction                |
| $\tau_{wy}$ | wave breaking stress in y direction                |





---

## Contents

---

|   | <i>Page</i> |
|---|-------------|
| <i>Title page</i>   |             |
| <i>Contract</i>   |             |
| <i>Summary</i>  |             |
| <i>List of symbols</i>  |             |
| <i>Contents</i>   |             |
| <br>  |             |
| <b>1 Introduction</b> .....   | <b>1</b>    |
| <b>2 Resume of work carried out in year one</b> .....   | <b>1</b>    |
| <b>3 Further Developments to PISCES</b> .....   | <b>2</b>    |
| 3.1 Conversion for serial computers .....   | 3           |
| 3.2 Inclusion of a non-equilibrium sand transport<br>model .....                              | 3           |
| 3.3 Tidal and wave driven forces and boundary<br>specification .....                          | 3           |
| 3.3.1 <i>Methodology</i> .....  | 3           |
| 3.3.2 <i>Derivation of wave-driven currents at the<br/>          lateral boundaries</i> ..... | 4           |
| 3.4 Incorporation of a space- and time-dependent eddy<br>viscosity .....                      | 5           |
| <b>4 Application of the model</b> .....   | <b>6</b>    |
| 4.1 Silver Strand Beach .....   | 6           |
| 4.1.1 <i>Introduction</i> .....   | 6           |
| 4.1.2 <i>Model layout</i> .....   | 6           |
| 4.1.3 <i>Model simulation</i> .....   | 6           |
| 4.2 River outflow with waves and tidal currents .....   | 7           |
| 4.2.1 <i>Introduction</i> .....   | 7           |
| 4.2.2 <i>Model Layout</i> .....   | 7           |
| 4.2.3 <i>Model simulation</i> .....   | 7           |
| 4.3 Keta Lagoon .....   | 8           |
| 4.3.1 <i>Introduction</i> .....   | 8           |
| 4.3.2 <i>Model setup</i> .....  | 8           |
| 4.3.3 <i>Model simulation</i> .....   | 8           |
| 4.4 Detached Breakwater .....   | 10          |
| 4.4.1 <i>Introduction</i> .....   | 10          |
| 4.4.2 <i>Model set-up and parameters</i> .....  | 10          |
| 4.4.3 <i>Application of PISCES</i> .....  | 10          |
| 4.4.4 <i>Model results</i> .....  | 11          |
| <b>5 Conclusions</b> .....  | <b>12</b>   |
| <b>6 Acknowledgments</b> .....  | <b>13</b>   |
| <b>7 References</b> .....   | <b>14</b>   |



---

## Contents continued

---

### Figures

|           |  |
|-----------|--|
| Figure 1  | 10m Silver Strand model  |
| Figure 2  | Silver Strand, waves 37 degrees, wave breaking stress over initial bed (every vector plotted)  |
| Figure 3  | Silver Strand, waves 37 degrees, wave orbital velocity over initial bed (every other vector plotted)   |
| Figure 4  | Silver Strand velocity field, waves 37 degrees, peak ebb   |
| Figure 5  | Silver Strand velocity field, waves 37 degrees, peak flood   |
| Figure 6  | Silver Strand, tidal residual sand transport field, vicinity of disposal mound, wave direction 37N   |
| Figure 7  | Silver Strand, tidal residual sand transport, vicinity of disposal mound, wave direction 37N   |
| Figure 8  | Silver strand, waves 77 degrees, wave breaking stress over initial bed (every vector plotted)  |
| Figure 9  | Silver Strand, waves 77 degrees, wave orbital velocity over initial bed (every other vector plotted)   |
| Figure 10 | Silver Strand velocity field, waves 77 degrees, peak ebb   |
| Figure 11 | Silver Strand velocity field, waves 77 degrees, peak flood   |
| Figure 12 | Silver Strand, tidal residual sand transport field, vicinity of disposal mound, wave direction 77N   |
| Figure 13 | Silver Strand, tidal residual sand transport, vicinity of disposal mound, wave direction 77N   |
| Figure 14 | River outflow test case; flow vectors, combined tidal and wave-driven currents, and river discharge  |
| Figure 15 | Location of Keta Lagoon, Ghana   |
| Figure 16 | Keta Lagoon model layout   |
| Figure 17 | Keta Lagoon test case, velocity field, HW+6 hours  |
| Figure 18 | Keta Lagoon test case, velocity field, HW+12.4 hours   |
| Figure 19 | Keta Lagoon study, rate of bed level change - static bed, HW+6 hours   |
| Figure 20 | Keta Lagoon study, rate of bed level change - static bed, HW+12.4 hours  |
| Figure 21 | A) Updated bed after 9 tides<br>B) Initial bathymetry<br>C) Physical model bathymetry after 170 hours<br>D) After 1 tide, intertidal update<br>E) After 1 tide, tidal update |
| Figure 22 | Detached breakwater, initial wave heights  |
| Figure 23 | Detached breakwater, initial current field   |
| Figure 24 | Detached breakwater, bed levels after 200 hours, 250 micron sand.  |
| Figure 25 | Detached breakwater, bedlevels after 200 hours, 100 micron sand  |

### Appendix Description of the SANDFLOW-2D model



---

## **1 Introduction**

---

This report describes the development and application of a fully interactive numerical model of the distribution of waves and currents, the resulting sediment transport, and the response of the coastline and coastal bathymetry, in complex coastal areas. The model, named PISCES, is based on existing models at HR Wallingford (HR) for waves and currents separately, complemented by recent advances in the understanding of sediment transport in such conditions. The model is capable of predicting the response of a complex coastal area both to engineering works and to natural changes such as rising sea level.

The model development work was commissioned by the Ministry of Agriculture, Fisheries and Food to cover a period of three years starting in January 1992. The applications of the model to specific test cases described herein were funded by the Commission of the European Communities Directorate General for Science, Research and Development as part of the G8M Coastal Morphodynamics research programme.

This report describes work carried out throughout the entire project. A short summary of work carried out in year 1 and reported in Chesher et al, 1993 is given in Chapter 2. Chapter 3 contains a description of all the project work with greater detail to model development in years two and three. Chapter 4 contains the results of various test cases to which PISCES has been applied in years two and three. A summary and conclusions from the full project are provided in Chapter 5.

---

## **2 Resume of work carried out in year one**

---

During the first year of this study the morphodynamic model was designed, built and tested against a variety of test cases. A full description of the work involved is given in Chesher et al, 1993, and a short resume is presented below.

The full morphodynamic model comprises four main sub-modules of wave propagation, current (wave-driven and tidal) distribution, sediment transport distribution, and bathymetric updating, and is based on the HR Wallingford TIDEWAY numerical modelling suite.

At the design stage it was considered prudent to make use of the existing, but separate, models for waves, currents and sediment transport, and to link them dynamically with a new morphodynamic updating routine. This approach makes the best use of well-established models with long pedigrees, and integrates them into one overall shell. The disadvantage of this approach is the need for frequent file input and output from each module, which can be computationally expensive, although this is not considered a large time-penalty in comparison with the overall runtime of the model.

Another feature of the model is that all morphodynamic simulations are completely automatic, with the user simply specifying the duration of the simulation required. Clearly, even time-independent hydrodynamic forcing gives rise to a time-dependent response in the bathymetry (such as in the propagation of an isolated dune in a steady current field), and PISCES



calculates automatically the optimum timestep required to maintain stability of the seabed so that model applications are simulated as efficiently as possible.

The model was tested against a number of scenarios:

- A flat bed case where due to the slope in the free surface the current speed increases with downstream distance. PISCES accurately predicted the equilibrium final bed configuration consisting of a sloping bed equal to the free-surface slope to maintain uniform currents over the domain.
- The deformation of a 1-D dune was accurately modelled up to the point where a shock should form, and inclusion of a gravity term to account for gradients of the seabed yielded a more realistic evolution of the dune.
- The 1-D dune problem was extended to 2-D, where it was seen that the model responds in a completely different way to that in the 1-D case. As well as propagating downstream, the dune spreads out laterally as a consequence of the interaction between the seabed and the free-surface. The evolution of the dune was compared with an analytical solution and gave broadly similar results.
- With the involvement of HR in the EC-funded MAST-G6M Coastal Morphodynamics research programme two further tests were simulated, allowing intercomparisons between the participating institutes. Cases of a river discharging into a wave-driven current field, and a semicircular bay under wave-driven currents were tested (de Vriend et al, 1993). In both cases PISCES gave comparable *initial* results to those from the other institutes, whereas the time-evolution of PISCES indicated a much more dynamic response. Such sensitivity highlights the need for a greater understanding of the behaviour of the sediment transport field in coastal systems.
- For the case of a semicircular bay, PISCES agreed reasonably well with results from a physical model of the study.

A good deal of progress was made in the first year. The remainder of the study was spent in improving the existing modules, enhancing the interactions between each module (eg inclusion of wave-breaking dissipation in the current module), and applying the model to further simulations. By these means a greater understanding of these complex morphological systems has been achieved, and PISCES is proving a valuable tool for investigating the response of the coastal environment to a variety of natural situations and human interferences.

---

### **3 Further Developments to PISCES**

---

Since the inception of the PISCES model, various changes and additions have been made. These have come about because of either hardware requirements or from the need to include more physical processes. This chapter describes various developments to PISCES which have taken place since the first report (Chesher et. al., 1993).



### **3.1 Conversion for serial computers**

PISCES originally ran on a parallel processing computer at HR called a DAP, standing for "Distributed Array of Processors". As such the coding was specifically designed to make use of this parallel computing, and the current module used an explicit finite difference method. With improvements in computing hardware, especially the increase in speed of serial computers, run times are now comparable between these two types of computer, and there is also the advantage of greater flexibility and portability in using serial machines.

The current module was converted to run on serial computers by making use of the Alternating Direction Implicit (ADI) version of TIDEFLOW-2D. Amendments that had been made to the explicit model to run in PISCES were incorporated into the ADI version. The potential sand transport model also ran on the DAP computer, so this also needed to be updated to run on a serial computer. At the same time it was decided to have the option to use a non-equilibrium sand transport model, and this is described in Section 2.2.

### **3.2 Inclusion of a non-equilibrium sand transport model**

Previously, PISCES had been run using a potential sand transport model, SAT. Whilst being converted to run on serial computers, PISCES was modified to have the option to run with a non-equilibrium sand transport module in order to include some quasi-three-dimensional (Q3D) effects whilst still maintaining computational efficiency. A lag function is included into the sand transport module to account for the time taken to pick up and set down the suspended sediment, which is directly related to the grain size.

These developments have had some important repercussions on the application of the model:

- It increases the run-time of applications, since the sand transport module requires the solution of a concentration equation which has a limiting timestep associated with it. Recall from year 1 that with the potential sand transport module the fluxes were derived from the flux rates and the morphological timestep in one operation.
- As with the current and wave modules, initial starting fields of suspended sediment concentrations must be calculated to limit the sediment pick-up at the start of the simulation.
- The initial mass of sand deposits must be specified, and for long simulations enough sand to prevent the formation of areas of hard bed is required. Although slightly more expensive to run, it is believed that this enhancement gives more realistic results, whilst still allowing relatively long simulations to be carried out.

### **3.3 Tidal and wave driven forces and boundary specification**

#### **3.3.1 Methodology**

In the past, PISCES had only been used on non-tidal problems, involving wave-driven currents only. It was necessary to develop PISCES further so that tidal motion could also be included. This section describes the methodology that was used, and its application is described in section 4.2.



Tidal motion is simulated by explicitly defining a time history of water levels and/or flow velocities at the appropriate boundaries (for large area models it is possible to drive the tidal models with elevation boundaries alone). Wave-driven currents are calculated at each interior model cell by inclusion of wave radiation stresses and orbital velocities in the horizontal momentum equations, and also by estimating the appropriate wave-driven current and water level setup at the model velocity and elevation boundaries respectively. Combined wave plus tidal motion is simulated by combining the contributions from waves and tides at the boundaries.

For general applications of the model the wave fields are passed to the current module, which integrates forward in time for one storage interval of the boundary file (the file containing velocities and elevations at the appropriate model boundaries which are stored typically at 10-15 minutes intervals), linearly interpolating in time between successive boundary values. The elevation field is then passed back to the wave module and the wave fields are redetermined. By this means the wave fields are calculated at the true water depths, and if the offshore wave input conditions change through the tide this can also be taken into account. Further developments including wave refraction in strong current gradients, and other wave-current interactions are possible with this architecture.

The horizontal velocity and elevation fields are typically stored at the same storage interval for later post-processing if required.

### 3.3.2 Derivation of wave-driven currents at the lateral boundaries

Previously, estimation of the wave-driven currents at the model lateral boundaries was made via a reduction of the appropriate momentum equation, assuming longshore uniformity, negligible cross-shore flow and viscous effects (see for example Chesher et. al. 1993). In the course of work carried out on various test cases, using this approach, an erroneous non-uniform behaviour of the flows near boundaries was observed, giving rise to associated bed level changes. It was found necessary to include the viscous effects (diffusion terms) for applications that included non-zero values of the horizontal diffusion coefficient, and this development resulted in homogeneous flows along streamlines near the boundaries with negligible apparent error. The revised method is described as follows:

Consider the equation for continuity of momentum for both components of the velocity field (ignoring Coriolis effects):

$$\frac{\partial u}{\partial t} + u \frac{\partial u}{\partial x} + v \frac{\partial u}{\partial y} = -g \frac{\partial z}{\partial x} - \frac{\tau_{bx}}{\rho d} + D \left[ \frac{\partial^2 u}{\partial x^2} + \frac{\partial^2 u}{\partial y^2} \right] + \frac{\tau_{wx}}{\rho d} \quad (1)$$

$$\frac{\partial v}{\partial t} + u \frac{\partial v}{\partial x} + v \frac{\partial v}{\partial y} = -g \frac{\partial z}{\partial y} - \frac{\tau_{by}}{\rho d} + D \left[ \frac{\partial^2 v}{\partial x^2} + \frac{\partial^2 v}{\partial y^2} \right] + \frac{\tau_{wy}}{\rho d} \quad (2)$$

where u, v are the velocity components in the x-,y- direction (m/s)

g is the acceleration due to gravity (m/s<sup>2</sup>)

z is the free-surface elevation (m)

$\tau_{bx}$ ,  $\tau_{by}$  are the bed shear stress components (N/m<sup>2</sup>)

$\tau_{wx}$ ,  $\tau_{wy}$  are the driving forces due to waves (N/m<sup>2</sup>)



$\rho$  is the water density (kg/m<sup>3</sup>)

$d$  is the water depth (m)

$D$  is the horizontal eddy diffusion coefficient (m<sup>2</sup>/s)

Consider an anti-clockwise coordinate system with x-axis normal to the coast. The assumptions of steady flow, longshore uniformity and negligible cross-shore mean flow reduce (1) and (2) to:

$$0 = -g \frac{\partial z}{\partial x} + \frac{\tau_{wx}}{\rho d} \quad (3)$$

$$0 = -g \frac{\partial z}{\partial y} - \frac{\tau_{by}}{\rho d} + D \frac{\partial^2 v}{\partial x^2} + \frac{\tau_{wy}}{\rho d} \quad (4)$$

Equation (3) is solved to define the cross-shore mean water level setup  $z$  (by assuming zero setup offshore). Equation (4) is solved numerically to define the longshore wave-driven current, using a Newton-Raphson method. Solution to (4) to an acceptable accuracy is very fast, requiring of the order of 10 iterations starting from an initial estimate of  $v$  based on the analytical solution to (4) without the diffusion term.

### 3.4 Incorporation of a space- and time-dependent eddy viscosity

Traditionally, the current module of PISCES, which is based upon the TIDEFLOW-2D model, used a constant horizontal eddy viscosity coefficient over the whole domain being modelled. Initial values for this coefficient are estimated according to:

$$D \approx (\text{mean velocity}) \times (\text{mean depth}) \quad (5)$$

This is sufficient for tidal currents to which TIDEFLOW-2D is applied, and adjustments to this value are usually made at the calibration stage in order to match observations of eddy sizes, current speeds etc. In the case of PISCES, where wave induced currents are very important it was deemed necessary to add some extra terms to the calculation of eddy viscosity to take into account the effect of waves, especially when the waves are breaking. Battjes (1983) related the horizontal eddy viscosity to the mean rate of wave-energy dissipation per unit area,  $D$  as;

$$v = M d (D/\rho)^{1/3} \quad (6)$$

where  $M$  is an empirical constant.

De Vriend and Stive (1987) used this term along with a term similar to equation (5) above in a heuristic approach, expressing the eddy viscosity as;

$$v = \kappa U \cdot d + M d (D/\rho)^{1/3} \quad (7)$$

where  $\kappa$  and  $M$  are constants,  $U$  is the frictional velocity,  $D$  is the rate of wave energy dissipation per unit area and  $\rho$  is the water density. This approach has been incorporated into PISCES, so that the eddy viscosity is now dependent on both current speed and wave-energy dissipation.



The wave module calculates the breaking wave energy dissipation and passes this value to the current module in the form of x,y arrays, in the same way that it passes information about wave orbital velocities, etc. The current module has a user supplied option either to use a constant eddy viscosity or calculate one from the dissipation information it receives from the wave module. The wave dissipation part of equation (7) has a peak value at the point where the waves break. A lower threshold for the eddy viscosity is needed so that in areas of low current and low wave dissipation (for example in very shallow water) the eddy viscosity does not tend to zero since a minimum eddy viscosity is usually necessary to prevent instability in the flow module.

---

## **4 Application of the model**

---

In order to ascertain the performance of the model with the inclusion of the developments described in Chapter 3, various test cases were run. This chapter describes the various cases and presents the results obtained.

### **4.1 Silver Strand Beach**

#### **4.1.1 Introduction**

A model evaluation exercise was undertaken with berm monitoring data from Silver Strand beach, California by Wallace and Chesher (1994). A coastal profile model (COSMOS) and an area model (PISCES), were used together so that both cross-shore and along-shore transport could be studied. The site is dominated by cross-shore processes which justifies the use of the profile model, but some small alongshore movements of the berm were also observed. PISCES was used to compare the *initial* deposition and erosion rates with observed longshore transport rates but, in view of the cross-shore dominant processes, the model was not run morphodynamically (the COSMOS model was run morphodynamically, and these results are presented in Wallace and Chesher, 1994).

#### **4.1.2 Model layout**

The model area was set up on a 10m grid, covering an area of 1240m alongshore by 800m in the cross-shore direction from the shoreline. Figure 1 shows the model area and bathymetry. A tide curve with range of 1.3m was imposed at the south eastern elevation boundary and the corresponding observed velocity was imposed at the north western velocity boundary. As well as the tidal driven currents, waves were also applied using the methodology described in Section 2.3. The nearshore profile had approximately a 1:45 slope, with an artificial sand berm of 300m longshore by 180m cross shore and an average relief of 2m in a depth of about 5m.

#### **4.1.3 Model simulation**

Two different wave conditions were tested. Condition 1 was with waves travelling at 37° to north and condition 2 was with waves at 77°. Both wave conditions had a wave period of 14 seconds. The wave and current modules were run interactively for the duration of a tidal period (for Condition 1 see Figures 2-7, for Condition 2 see Figures 8-13). Once a repeating tide had been obtained the sand transport module was run for one tide. Figures 2-7 show the predicted wave breaking stresses, wave orbital velocities, velocity fields at peak ebb and flood, residual sand transport and bed level changes over a tide for Condition 1. Figures 8-13 correspond to Condition 2. Gradients in transport rate over the berm are small, but resulted in some erosion at the southern end of the berm, equivalent to a sand loss of 300m<sup>3</sup>



of sand per tide. This corresponded well with measured sand losses over the survey period of 270m<sup>3</sup> per tide.

## **4.2 River outflow with waves and tidal currents**

### **4.2.1 Introduction**

In the first year report, various test cases were reported to which PISCES had been applied. These were all test cases involving steady wave-driven currents. The model has since been applied to a test case involving time-varying tidal currents (in addition to the steady wave-driven currents) based on the river outflow test case (Chesher et. al. 1993).

### **4.2.2 Model Layout**

The river outflow test case was used to demonstrate the *morphodynamic* predictions of PISCES and was described in Report SR337. It consists of a uniformly sloping beach of slope 1:50 from the coastline to a depth of 13.5m. The model covered an area of about 800m seawards by 1600m along the coast and comprised a regular 15m grid. A slightly deeper river channel extended perpendicularly from the coast.

### **4.2.3 Model simulation**

For the wave module the offshore boundary had a prescribed wave height and (peak) period of  $H_{ms}=2m$  and  $T=8s$  respectively, propagating at an angle of 30° (wave crest to the coastline).

This wave climate was superimposed on a tide of range 2m about mean sea level, defined at the top elevation boundary as a sinusoid, starting at high water and with a tidal period of 12.5 hours. At the offshore elevation boundary the water level is determined according to a linear interpolation between the defined levels at the top and bottom boundaries.

To calculate the tidal currents various aspects of the tidal motion are assumed that would normally be obtained from tide tables, viz. for this case the tidal range and mean tide level do not vary between the top and bottom boundary. The tidal currents along the bottom boundary are calculated by assuming a balance between the inertial pressure gradient and friction forces as described in Southgate (1989). Similarly, at the river mouth the tidal currents are calculated, and the equivalent tidal discharge is combined with the freshwater discharge to yield the net river flow.

Flow vectors through the tidal cycle are presented in Figure 14, which indicate that for the particular tide modelled the tidal current component inshore is small compared with the wave-driven contribution, so that the currents there are unidirectional. Likewise, the river flow is always seaward, with faster velocities at low water. Offshore, the wave-driven currents are much smaller and the flows are tidal-oscillatory. At low water (HW+6hrs) the cells adjacent to the coast dry out, and the peak current streamline, corresponding to a location close to the breaker point, moves offshore some thirty metres.



## 4.3 Keta Lagoon

### 4.3.1 Introduction

PISCES was applied to the study of a breach through a coastal sand strip, connecting a large lagoon with the Gulf of Guinea at Keta, Ghana (see Figure 15). This study formed part of an intercomparison exercise with other institutes as part of the MAST-G8M research programme, as well as with data from a physical model of the area.

### 4.3.2 Model setup

Data from the physical model study was used to define the numerical model specification. The bathymetry was supplied in digital form on a 15m grid, spanning the breach and extending some 1.5km along the coast, 450m offshore, and including a schematised lagoon as depicted in Figure 16. The conditions represented in the physical model comprised oblique wave attack giving rise to a longshore current, and tidal action. The tide was simulated by water level variations (schematised into a flood level and an ebb level) causing tidal flow into and out of the lagoon through the breach. Water levels in the lagoon were maintained at MWL. Tidal currents at the lateral boundaries were not represented; hence the boundary currents were wave-driven only. The wave data consisted of an offshore wave height,  $H_s$  of 1.96m, peak period,  $T_p$  of 8s and an offshore wave direction of  $15^\circ$  (wave crest to coastline). Data from the physical model comprised new bed levels after 170 hours (model scale, representing of the order of one year in nature) and the equivalent bed level changes over this period.

For the numerical model intercomparison the tide was represented by sinusoidal water level variations at the offshore boundary with a tidal period of 12hrs 25mins and a range of 0.98m (mean tide). The lateral boundaries had specified wave-driven currents only, for consistency with the physical model. All other hydrodynamic conditions were as above. The roughness length and coefficient of eddy diffusivity for momentum were specified as 0.1m and  $2.0\text{m}^2\text{s}^{-1}$  respectively, and the sediment had a median grain size,  $d_{50}$  of 0.54mm. The model was run using natural scale dimensions (not physical model scale dimensions).

The objective of the exercise (which is currently ongoing) is to run the model in morphodynamic mode for a relatively long period of approximately one year so that the bathymetric evolution obtained from each participating institute could be compared against the laboratory data. However, results to date comprise the initial hydrodynamic and transport fields and initial response of the model; the application of PISCES to the long-term forms part of a separate study.

### 4.3.3 Model simulation

Using the specified parameter settings the model was run over a static bed for two tides to allow the hydrodynamic fields to reach steady, repeating conditions. This involved the recalculation of new wave fields every 10 minutes, passing the water levels from the current module to the wave module, in order to simulate the correct wave breaking forces and wave orbital velocities to be passed back to the current module throughout the tidal cycle. The current flow vectors at times HW and HW+6hrs are presented in Figures 17 and 18, and these show the main processes of longshore currents in the coastal zone and tidal filling and emptying of the lagoon. The sediment flux field was calculated and the associated rates of bed level change at the same



times for the initial static bed are presented in Figures 19 and 20. These plots highlight the variation in the transport rates through the tide, in particular, just outside the breach where some points undergo strong accretion followed by erosion, or vice versa.

From these hotstart hydrodynamic conditions the morphodynamic simulation was carried out in a similar fashion, ie by running the hydrodynamic module for 10 minutes, calculating the sediment flux, and updating the bed accordingly. At each morphodynamic stage the optimum morphodynamic timestep consistent with a stable bed evolution was calculated based on the sediment fluxes, and compared to the imposed timestep (600s). In each case the imposed timestep was less than the optimum timestep, thus ensuring bathymetric stability.

The updated bathymetry after nine tides is presented in Figure 21a, alongside the initial bathymetry 21b. Comparison with the physical model bathymetry for 170 hours (approximately one year in nature, Figure 21c) indicates that, although further integration of the numerical model is necessary to simulate the correct period of evolution, the model is behaving at least qualitatively correctly. In general there is accretion on the upstream face of the channel associated with the breach and erosion on the downstream face.

Bed changes were greatest over the first tide, with some point depths changing by over 1 metre, whereas after nine tides the bed was evolving more slowly with only a few points varying by just over 0.5m per tide. However, within the tidal cycle the bed level changes may be greater than this. This aspect of the study has highlighted an important factor regarding the numerical modelling of the seabed evolution under the influence of strongly varying flow conditions, namely that of relating the timescale of the seabed evolution to that of the hydrodynamics. In particular, for this application, to run the model in this sub-tidal morphological mode is expensive and time-consuming, and raises a number of issues:

- (1) Is it necessary to update the bed through the tidal cycle, or would tidal residual fluxes (over a static bed) give a similar answer? The updated bathymetry after the first tide is presented in Figure 21d, and, as an intercomparison, this first tide was re-run, calculating tidal residual sediment fluxes, and the bed updated at the end of the tide, as shown in Figure 21e.
- (2) Figures 21d and e show that the computed bed levels differ according to the modelling approach. The question now is whether these differences are significant, causing the bathymetric evolutions to diverge, or whether after a suitable period of integration the solutions will converge.
- (3) On the longer timescale, can tidal residual fluxes be extrapolated, rather than recalculated after each tide? If so, what is the criterion for flow recalculation?

This study is being used to define an operational protocol, by defining various regimes for the morphological evolution, according to the timescale for the bathymetric changes, and applying the most appropriate integration procedure. For the test cases considered so far, where the initial conditions are far from equilibrium, the modelling approach would normally start with intra-tidal



bathymetric updating, changing to tidal updating after the timescale for bed changes has reduced, and finally to tidal extrapolation after further integration. However, the protocol should also allow a return to the intra-tidal updating procedure, should the hydrodynamic conditions change due to, for example, the onset of storm conditions.

One specific feature which is not represented in the model is the erosion of the channel sides. This was highlighted during the study of this test case, and with the other institutes running the same case. The erosion of these dry areas is now being looked at in more detail.

## **4.4 Detached Breakwater**

### **4.4.1 Introduction**

PISCES has been applied to the study of a detached breakwater. Intercomparison tests are currently being undertaken with a physical model situated at SOGREAH in Grenoble, France. These comparisons will allow the calibration of the wave driven currents in PISCES. In order to ascertain the response of the model, a preliminary investigation was undertaken using PISCES running in a morphodynamic mode. Model results using different grain sizes highlight the time lag effect inherent in the non-equilibrium sand transport module.

### **4.4.2 Model set-up and parameters**

An area of coast extending 1680 metres alongshore and 780 metres offshore was setup with a gently sloping 1:50 bed with an offshore bed level of 13.5m. A breakwater 150 metres long was placed along the 6.0m contour in the centre of the model area as shown in Figure 22. The flow module made use of a grid with cells 15m by 15m, whereas the wave module used cells 15m in the alongshore direction and 3m in the cross-shore direction. The water level within the model was set at 0.0m (MWL). All the boundaries were no-flow representing in effect, a closed basin.

Only wave-induced currents were included for this case. A roughness length of 0.05m and a diffusion coefficient of  $5\text{m}^2\text{s}^{-1}$  were used. An offshore wave height  $H_{\text{ms}}$  of 2.0m, peak period  $T_p$  of 8s and an offshore wave direction of  $0^\circ$  (wave crest parallel to coastline) were used.

Morphodynamic modelling was undertaken for two cases, each with the same parameters apart from the grain size represented in the sand transport model. The grain sizes used were  $250\mu\text{m}$  and  $100\mu\text{m}$ . These were chosen in order to examine the time lag effect (included in the non-equilibrium sand transport module) on the morphological behaviour.

### **4.4.3 Application of PISCES**

Each of the two morphological runs underwent the same process, that of calculating initial wave, current and sand flux fields with which to start the simulations, and then the main simulation itself. This process worked as follows:

Wave and current modules were run consecutively for ten minutes, updating the wave and current fields. The wave field is shown in Figure 22. This was repeated until the wave-driven currents reached a steady state solution (see Figure 23). The peak initial speed is about 0.9m/s along the back edge of the



breakwater. This process ensures a well defined starting condition with which to run the morphodynamic model.

Using the stored flow results, the non-equilibrium sand transport model was run for ten minutes in order to obtain starting conditions for the suspended and deposited sediment concentrations.

Using these start conditions the model was run morphologically for a period of 200 hours, during which time PISCES looped through the wave, current, sand transport and bed updating modules in turn, stepping through with a time step derived from the speed at which the bed was being updated.

#### 4.4.4 Model results

It was anticipated that the model, if behaving at all realistically, should produce a tombolo formation behind the breakwater. This was seen to be so, but the shape was seen to be sensitive to the grain size used.

For both grain sizes, a channel can be seen along the tombolo's axis of symmetry. This is caused by the convergence zone of the two eddies formed behind the breakwater. Tombolos have been observed to form when

$$\frac{L_s}{Y} \geq 1.0$$

where  $L_s$  is the length of the breakwater and  $Y$  is the distance offshore of the detached breakwater (Chasten, Rosati, McCormick and Randall, 1993). In the case of this model, the value of  $L_s/Y \approx 1.0$  and as such the formation lies on the border line between two salients and a tombolo.

By virtue of the lag effect included in the sediment transport module, finer sand particles stay in suspension longer than coarser ones. Figure 24 and 25 show the model bathymetry with  $250\mu\text{m}$  and  $100\mu\text{m}$  sand, respectively, after 200 hours. The larger grain size sand falls out of suspension more quickly than the finer sand, and this is evident if one compares the area directly behind the breakwater. Here, more of the finer sand has built up than the coarser sand which is due to the finer sand being held in suspension for longer and being carried right up to the breakwater wall.

A scouring effect can also be seen in Figures 24 and 25 at each end of the breakwater, caused by the strong current shear in this region. As the tombolo is formed, the eddy behind the breakwater migrates and sets up stronger offshore flows at either end of the breakwater, modifying the initial morphodynamic response.

Perturbations can be seen along the shoreline in Figures 24 and 25. These start to form when the eddy is moved from behind the breakwater and create secondary circulations.

These sets of tests have highlighted the sensitivity of the model to grain size and have given some indication that the model is producing results that are credible. Comparisons with the physical model at SOGREAH will now be undertaken in order to ascertain if the wave driven currents being produced can realistically represent those in the physical model. A full scale PISCES run of the physical model will also be run morphologically.



The inability for PISCES to erode dry land at the moment is also evident from the results of this test case. Areas along the shoreline on either side of the breakwater have been identified as places of erosion as the sediment from these areas is transported to make up the tombolo. This will be a useful test case for examining the dry erosion capability of PISCES as the relevant physics are included. It will also make a difference to the amount of material transported to form the tombolo.

---

## 5 Conclusions

---

1. During the first year of this study PISCES was designed, built and tested against a variety of test cases. The full morphodynamic model comprises four main sub-modules of wave propagation, current (wave-driven and tidal) distribution, sediment transport distribution, and bathymetric updating.
2. PISCES is an integrated, interactive model for use in coastal engineering and research projects. It offers the user a more detailed picture of the morphodynamic response of the study either through natural processes or human interference, by allowing the seabed to evolve according to the sediment dynamics. By this means the impact of, eg engineering schemes, can be more clearly interpreted than by simply analysing the *initial* response of the model.
3. An additional feature of the model is that all morphodynamic simulations are completely automatic, with the user simply specifying the duration of the simulation required. Automatic updating of the hydrodynamics is performed according to the internal morphodynamic timestep consistent with maintaining a stable seabed.
4. The model was tested against a number of scenarios. In each case the model behaved realistically, and in some applications (notably the river outflow case and the 2-D dune) very dynamic response of the model was obtained, which was either validated (2-D dune) or is the subject of further study (river).
5. In the last two years of this three-year study, PISCES has been converted to run on a serial computer. This will allow it to run on a wider range of computers in the future.
6. A non-equilibrium sand transport module has been developed as an alternative to the potential transport module described in the first year report (Chesher et. al. 1993). This can produce more realistic sand transport patterns, which will give rise to more accurate morphological predictions.
7. Time varying wave and tidal conditions can now be specified, allowing more site specific applications to be modelled along with steady conditions. The boundary specifications for these conditions were derived.
8. A spatially and time varying eddy viscosity has been incorporated to take into account increased mixing due to breaking waves. This can have a marked effect on current velocities within and close to the surf zone.



9. Comparisons with measured data from Silver Strand Beach, California and with results from a profile model have been made. Good correspondence was obtained between the initial measured and predicted erosion rates.
10. An application to a tidal lagoon at Keta, Ghana was studied. The morphodynamic evolution of the submerged channel associated with the breach was good. However, accurate simulation of the breach location requires the capability to erode the coastline. This aspect of the modelling is currently being investigated.
11. A simulation of tombolo formation behind a breakwater has been studied, showing qualitatively realistic results. The calibration of wave driven currents produced by PISCES is being undertaken by comparing with measurements made in a physical model.

---

## **6 Acknowledgments**

---

The authors would like to thank the members of the Marine Sediments Group at HR Wallingford for their help and advice, and also colleagues in the MAST G8M collaborative research group.

Figures 15 and 21c are reproduced courtesy of Delft Hydraulics.



---

## **7 References**

---

Battjes, J A (1983) Surf Zone Turbulence. Proc. 20th IAHR Congr., Moscow. Seminar of Hydrodynamics of Waves in Coastal Areas.

Chasten M A, Rosati J D, McCormick J W and Randall R E (1993). Engineering Design Guidance for Detached Breakwaters as Shoreline Stabilisation Structures. Technical Report CERC-93-19. pp38-48.

Chesher T J, Wallace H M, Meadowcroft I C, Southgate H N (1993). PISCES A Morphodynamic Coastal Area Model, First Annual Report. Report SR337, HR Wallingford (April).

De Vriend H J and Stive M J F (1987). Quasi-3D Modelling of Nearshore Currents. Coastal Engineering, 11 pp 565-601.

De Vriend HJ, Zyserman J, P  chon P, Roelvink JA, Southgate HN, Nicholson J (1993). Medium-Term 2DH Coastal Area Modelling. Coastal Engineering, 21 pp93-224.

Southgate H N (1989) A Nearshore Profile Model of Wave and Tidal Current Interaction, Coastal Engineering, Vol 13.

Wallace H M and Chesher T J (1994). Validation of Coastal Morphodynamic models with field Data. Coastal Dynamics '94, Barcelona.



## Figures



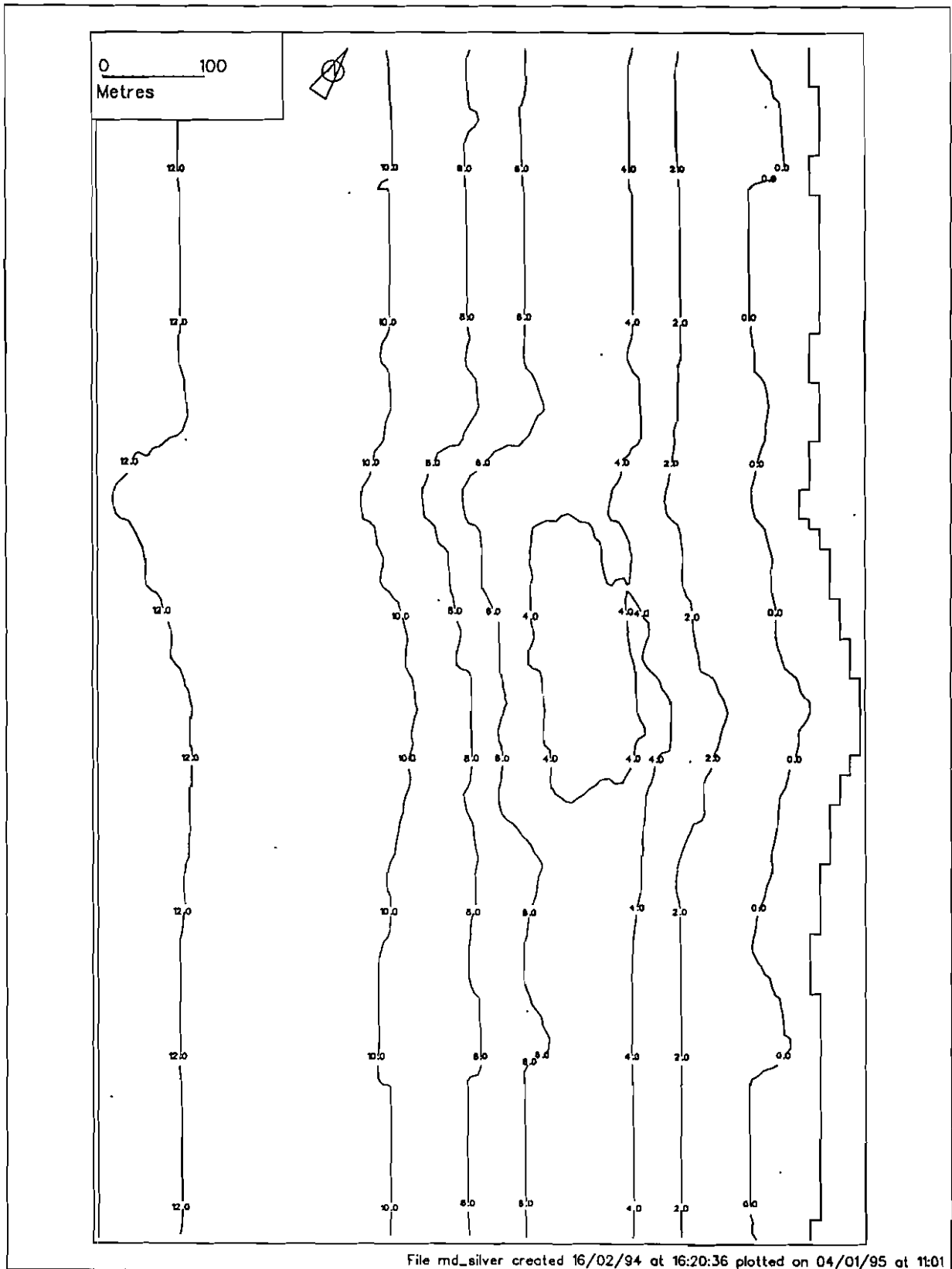


Figure 1 10m Silver Strand model

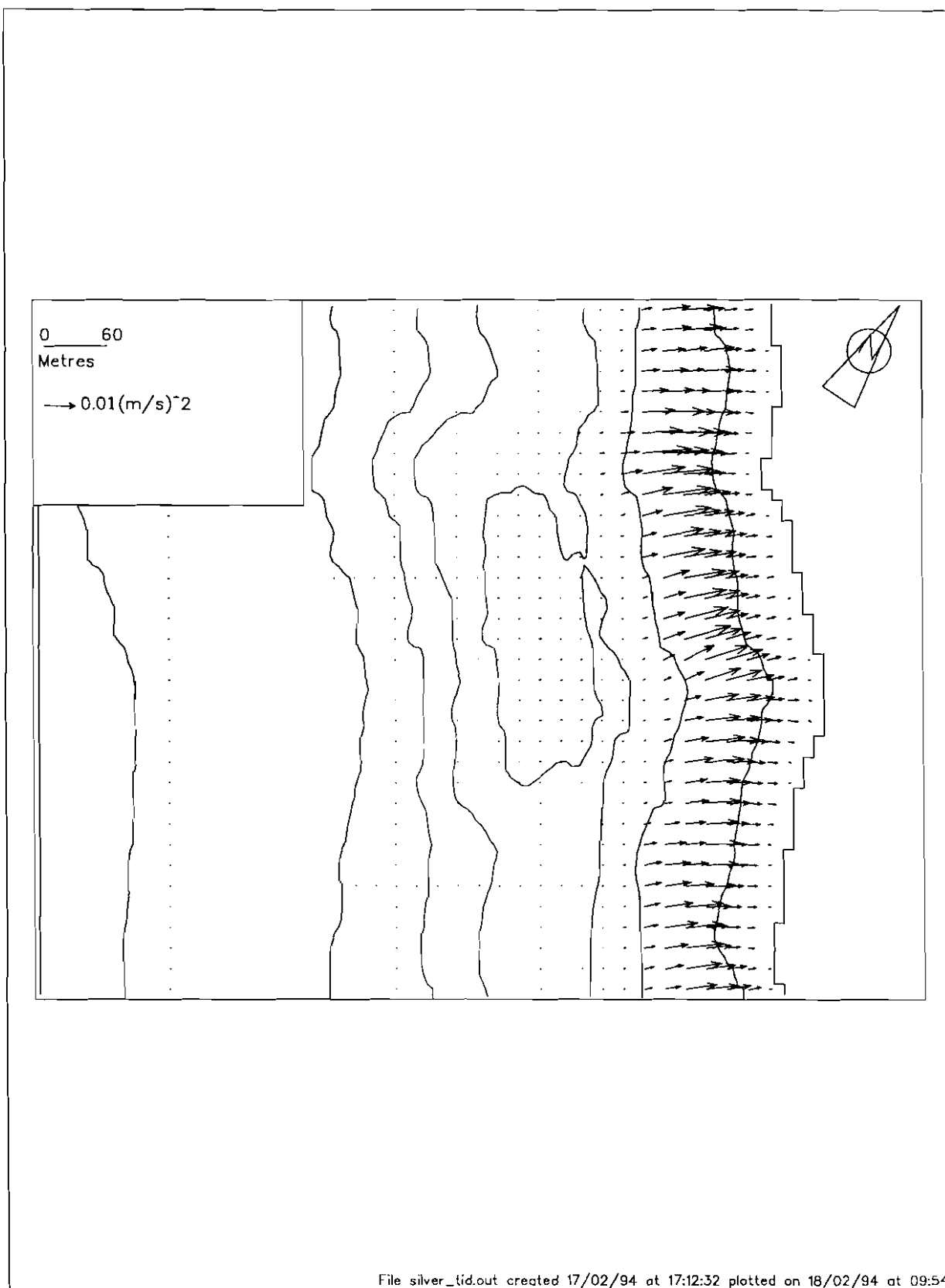


Figure 2 Silver Strand,waves 37 degrees  
Wave breaking stress over initial bed  
(every other vector plotted)

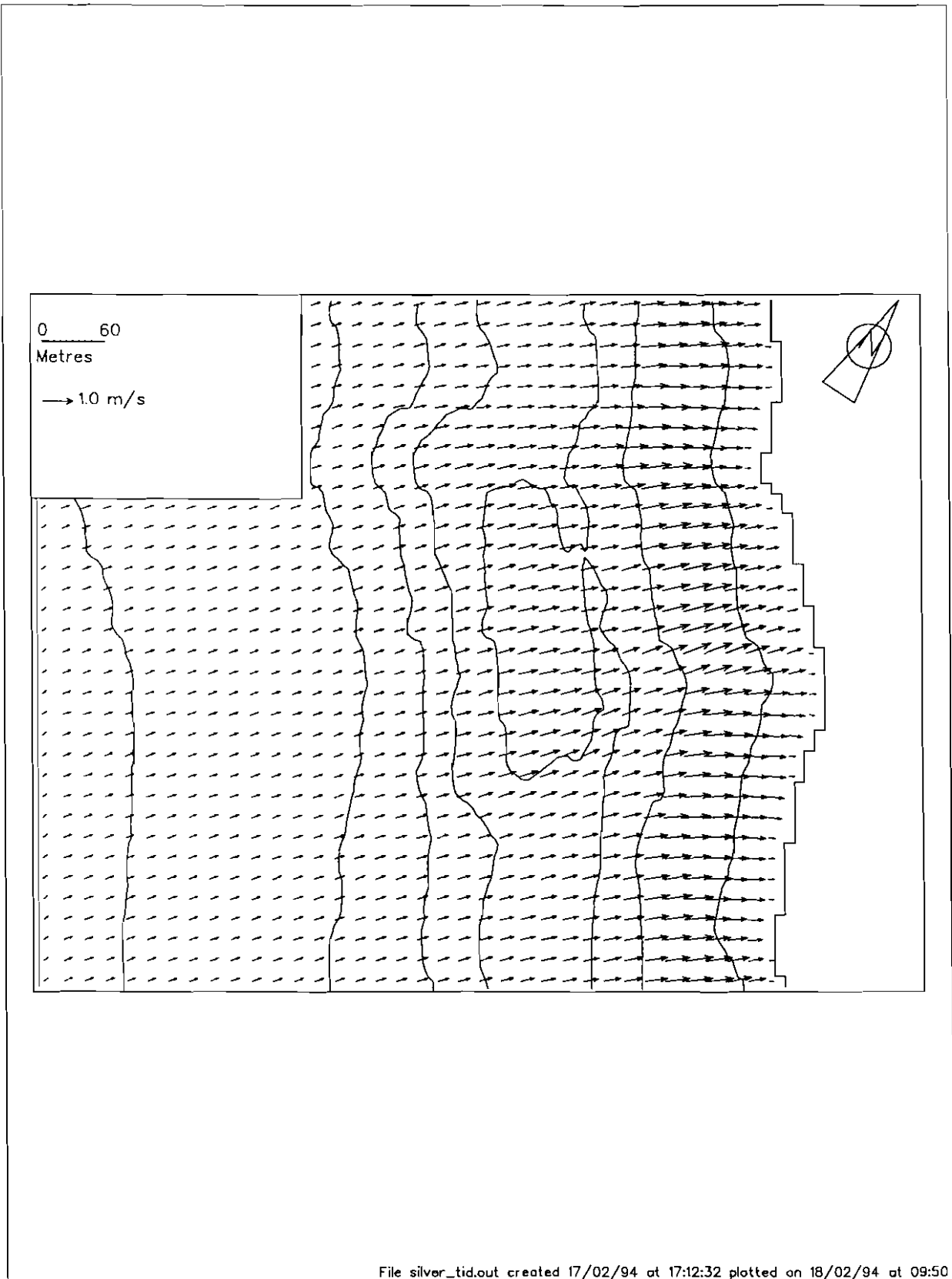


Figure 3 Silver Strand, waves 37 degrees  
Wave orbital velocity over initial bed  
(every other vector plotted)

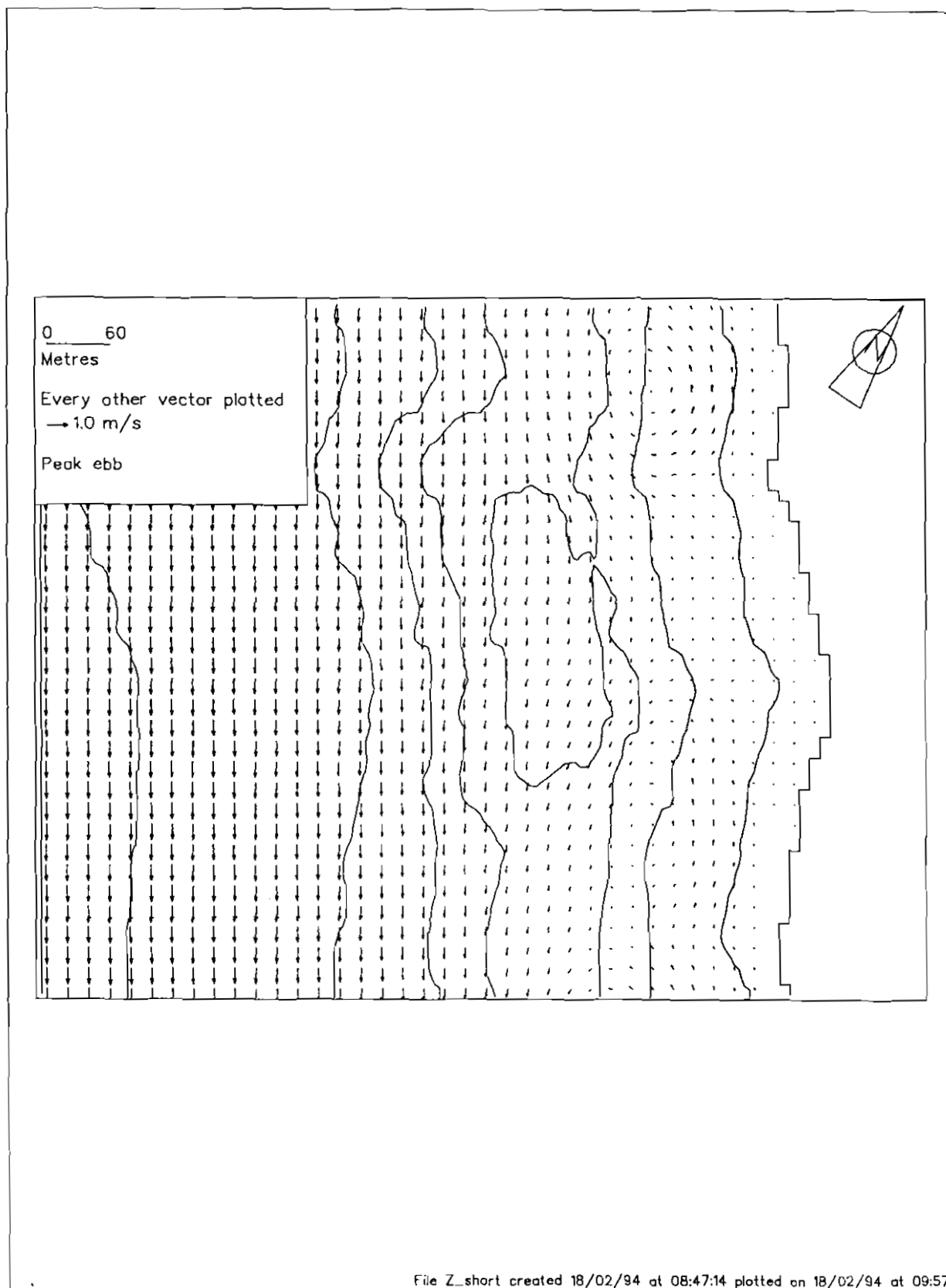


Figure 4 Silver Strand velocity field  
waves 37 degrees  
Peak ebb

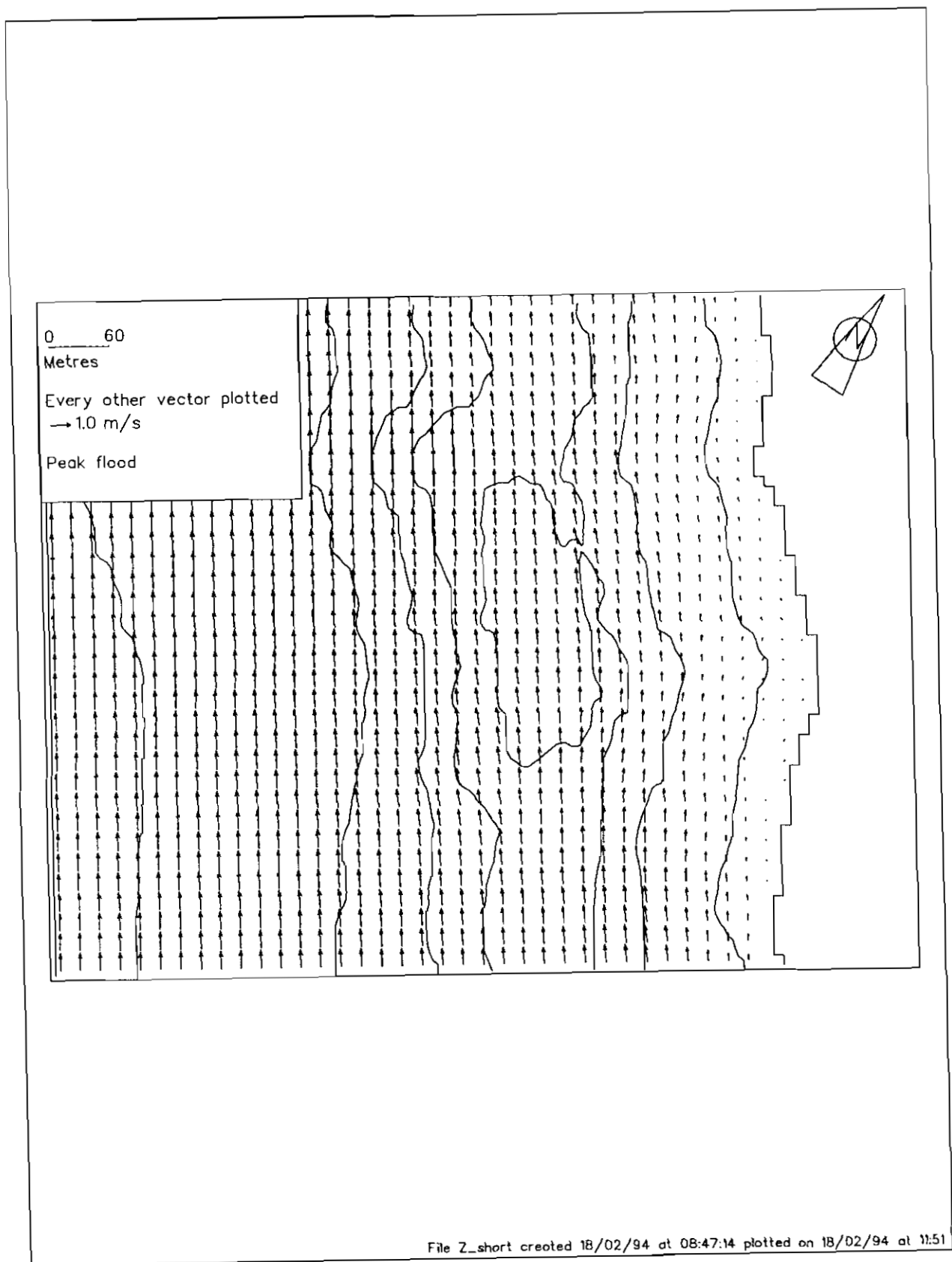


Figure 5 Silver Strand velocity field  
waves 37 degrees  
Peak flood

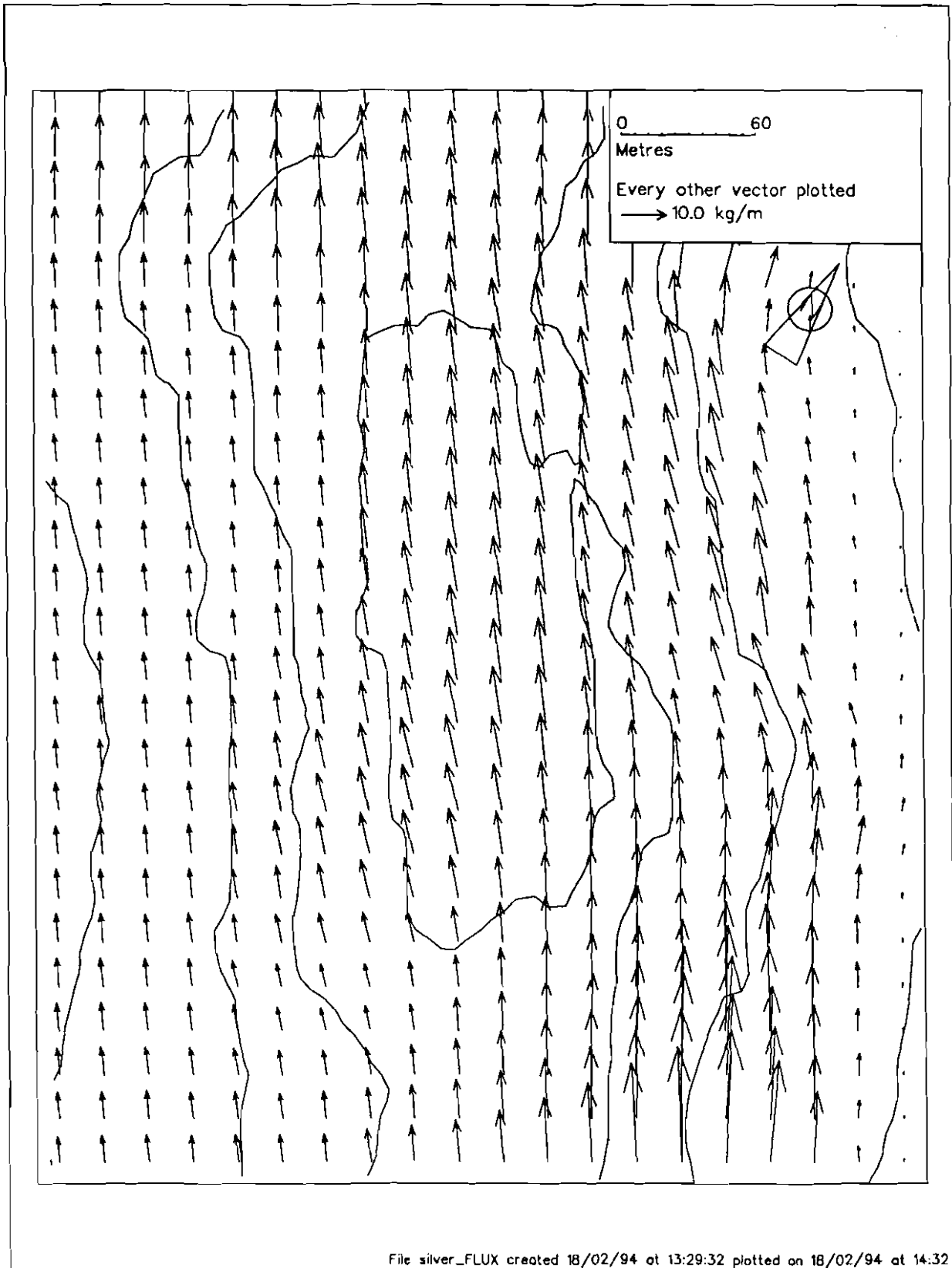


Figure 6 Silver Strand  
Tidal residual sand transport field  
Vicinity of disposal mound  
Wave direction 37 N

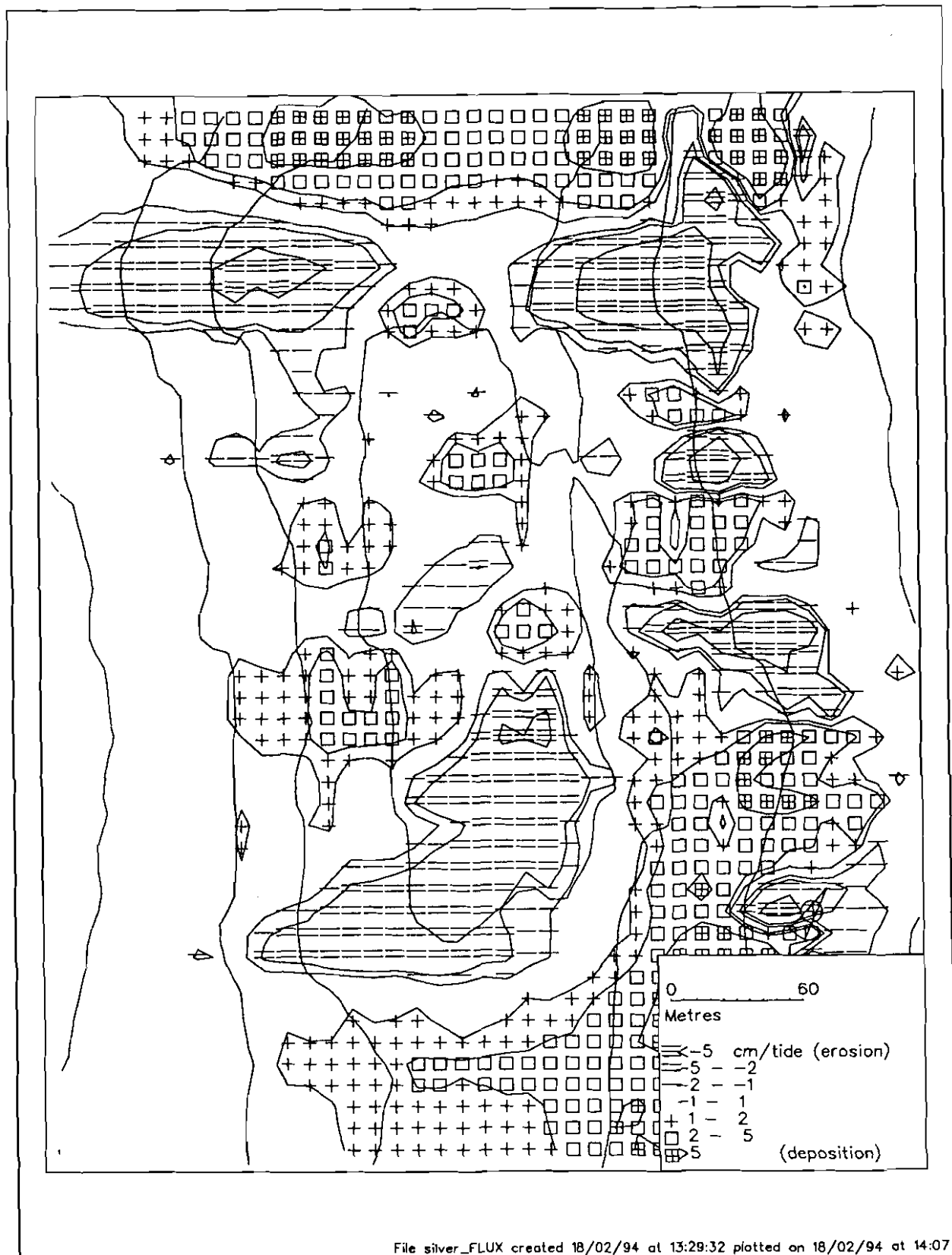


Figure 7 Silver Strand  
Tidal residual sand transport  
Vicinity of disposal mound  
Wave direction 37 N

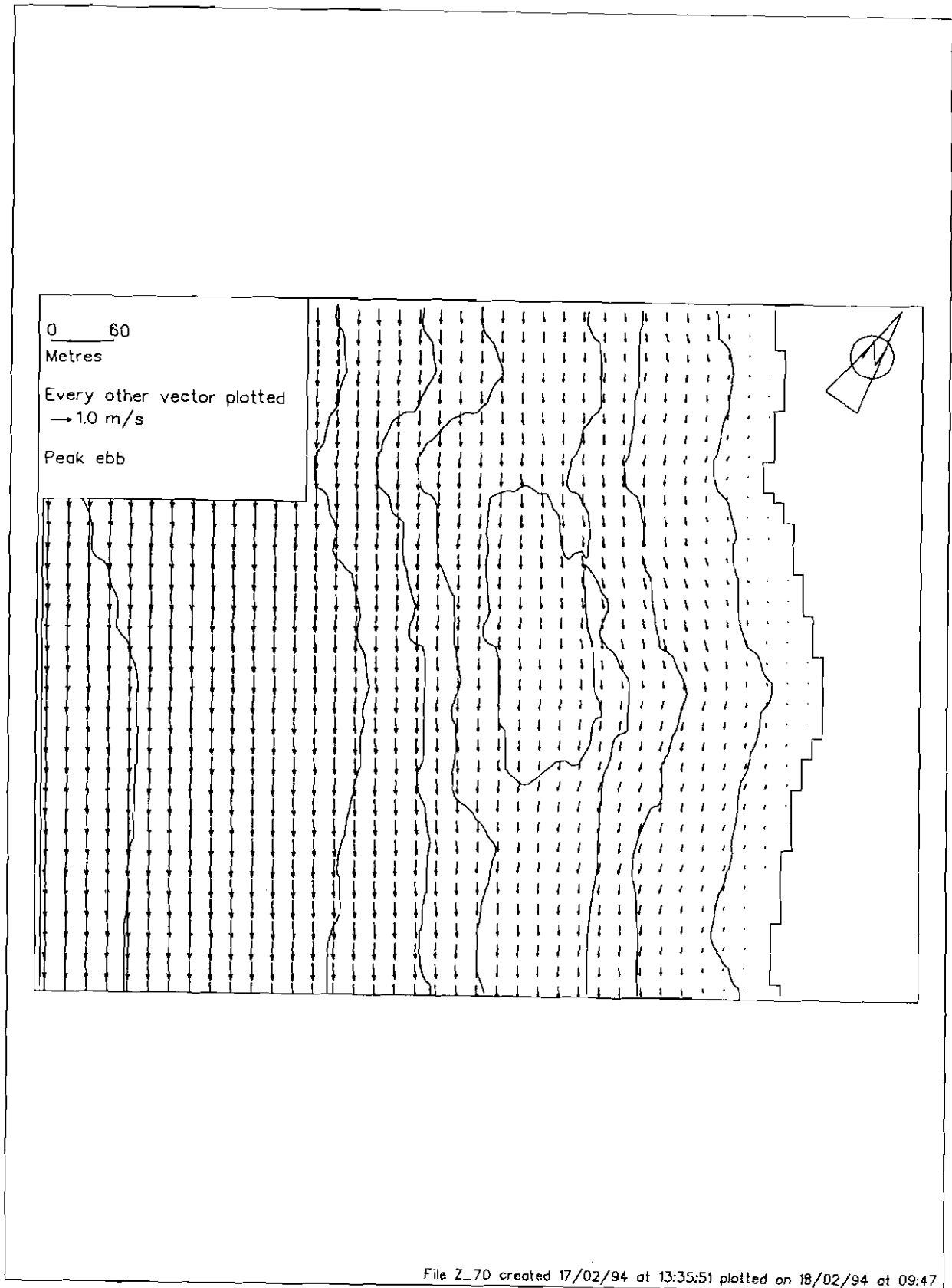


Figure 10 Silver Strand velocity field  
waves 77 degrees  
Peak ebb

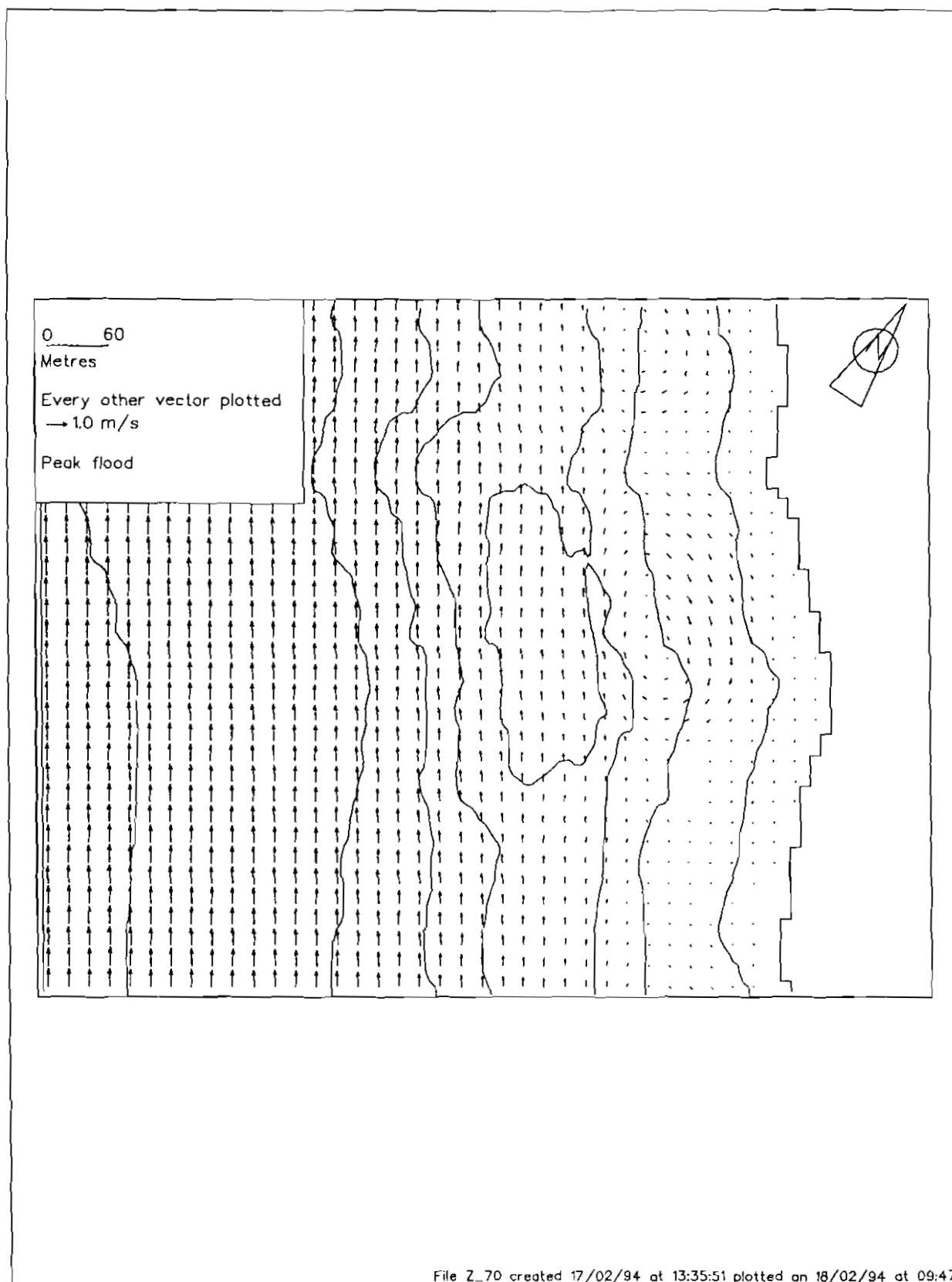


Figure 11 Silver Strand velocity field  
waves 77 degrees  
Peak flood

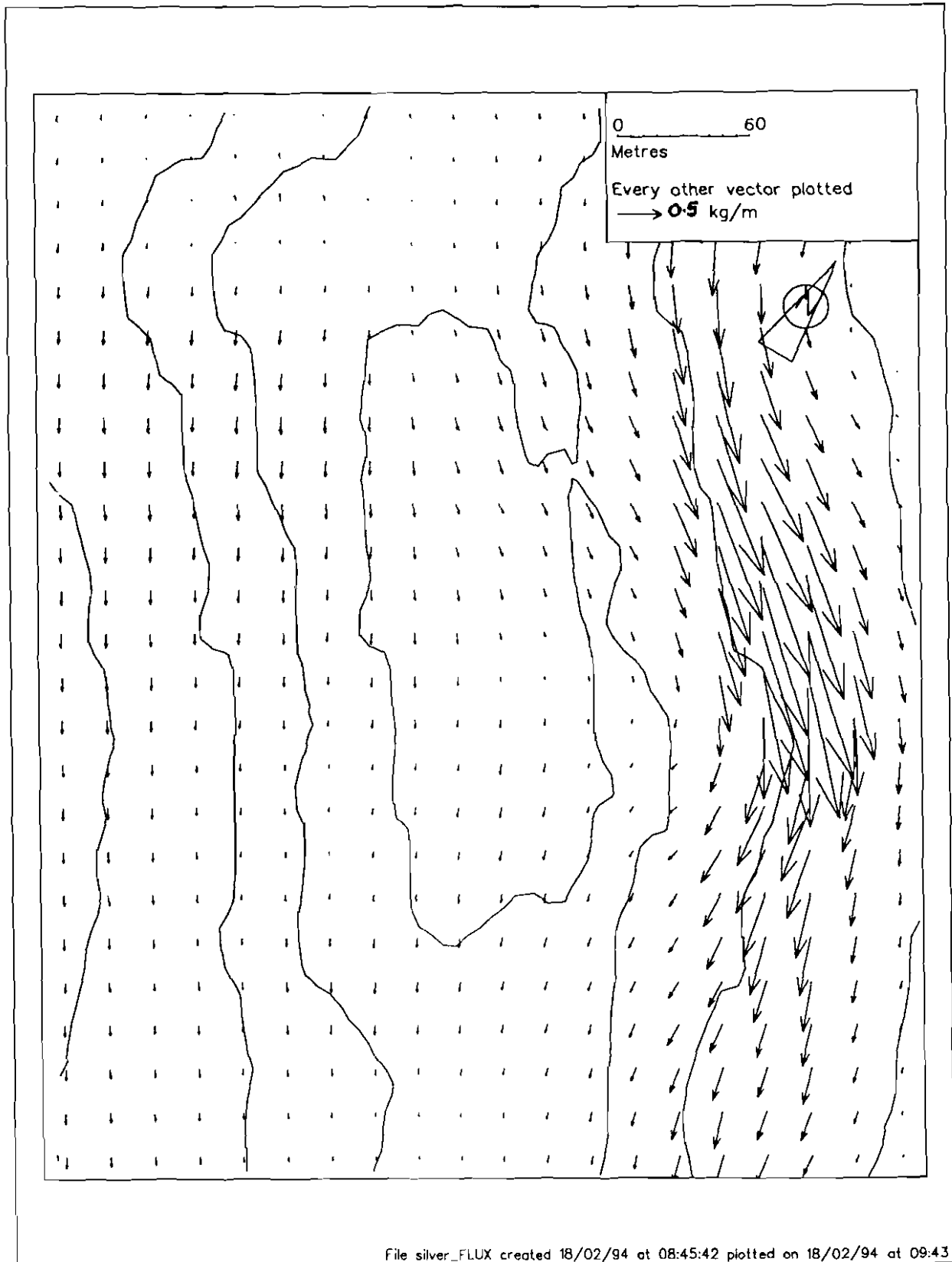


Figure 12 Silver Strand  
Tidal residual sand transport field  
Vicinity of disposal mound  
Wave direction 77 N

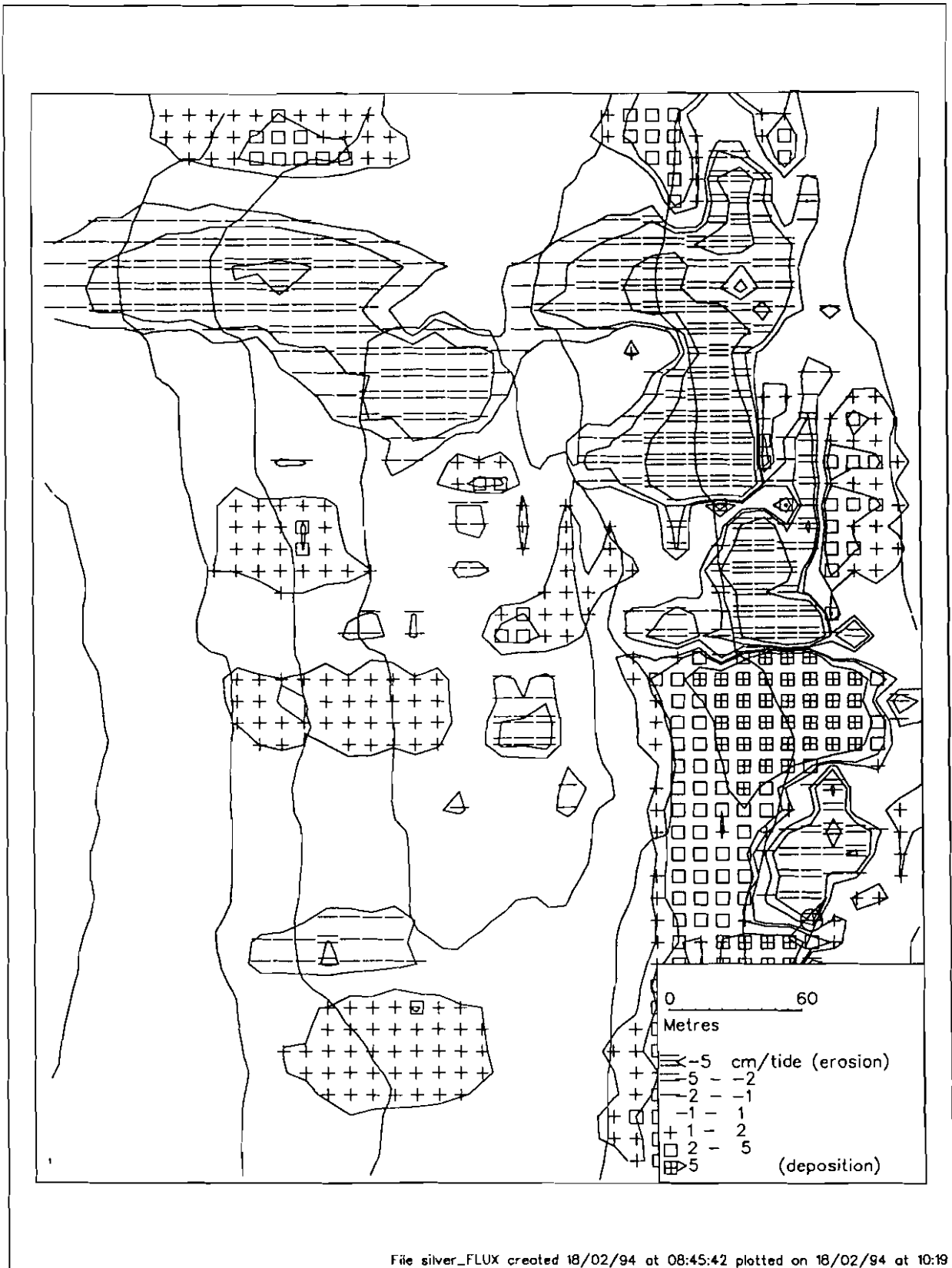
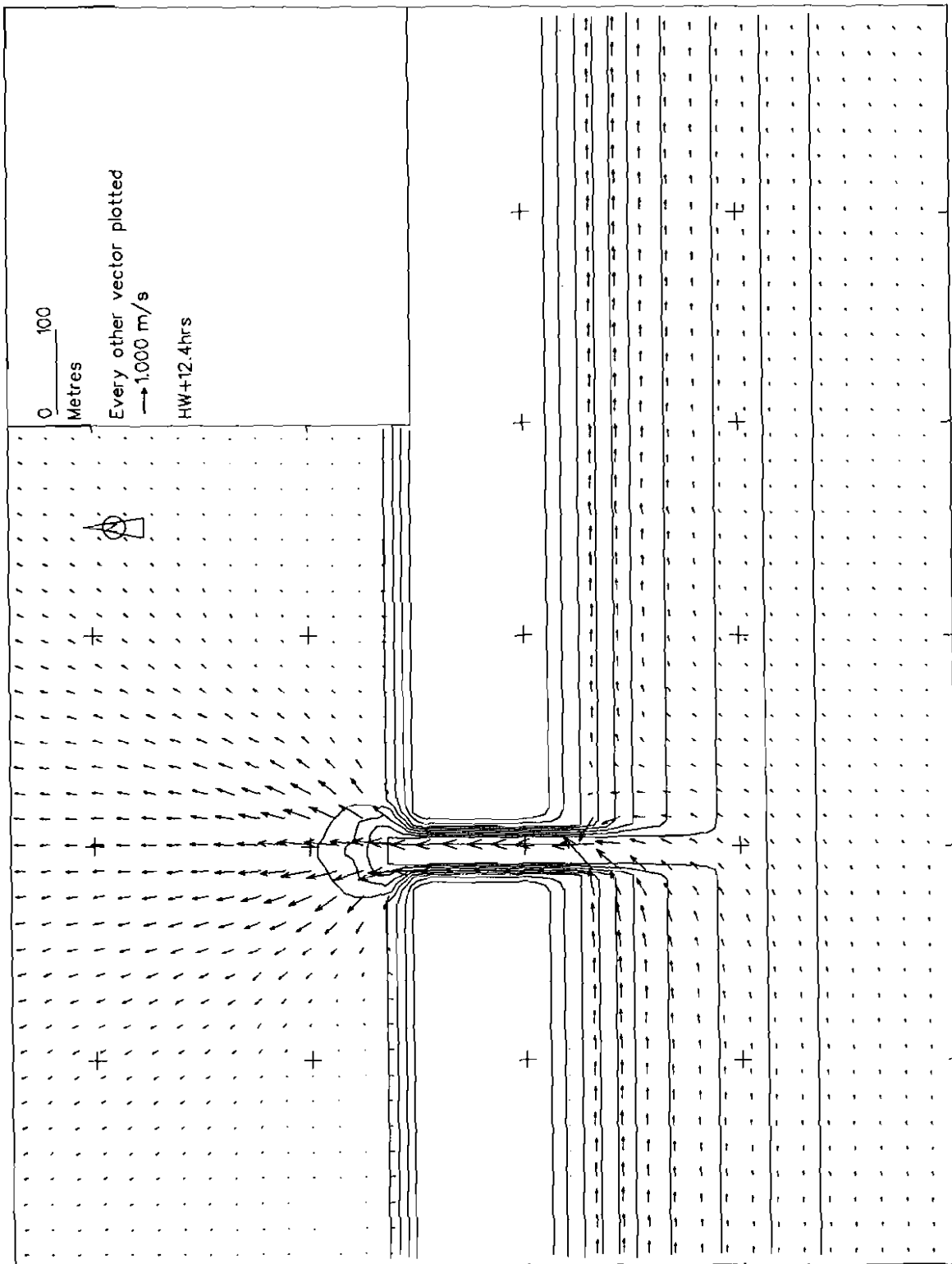
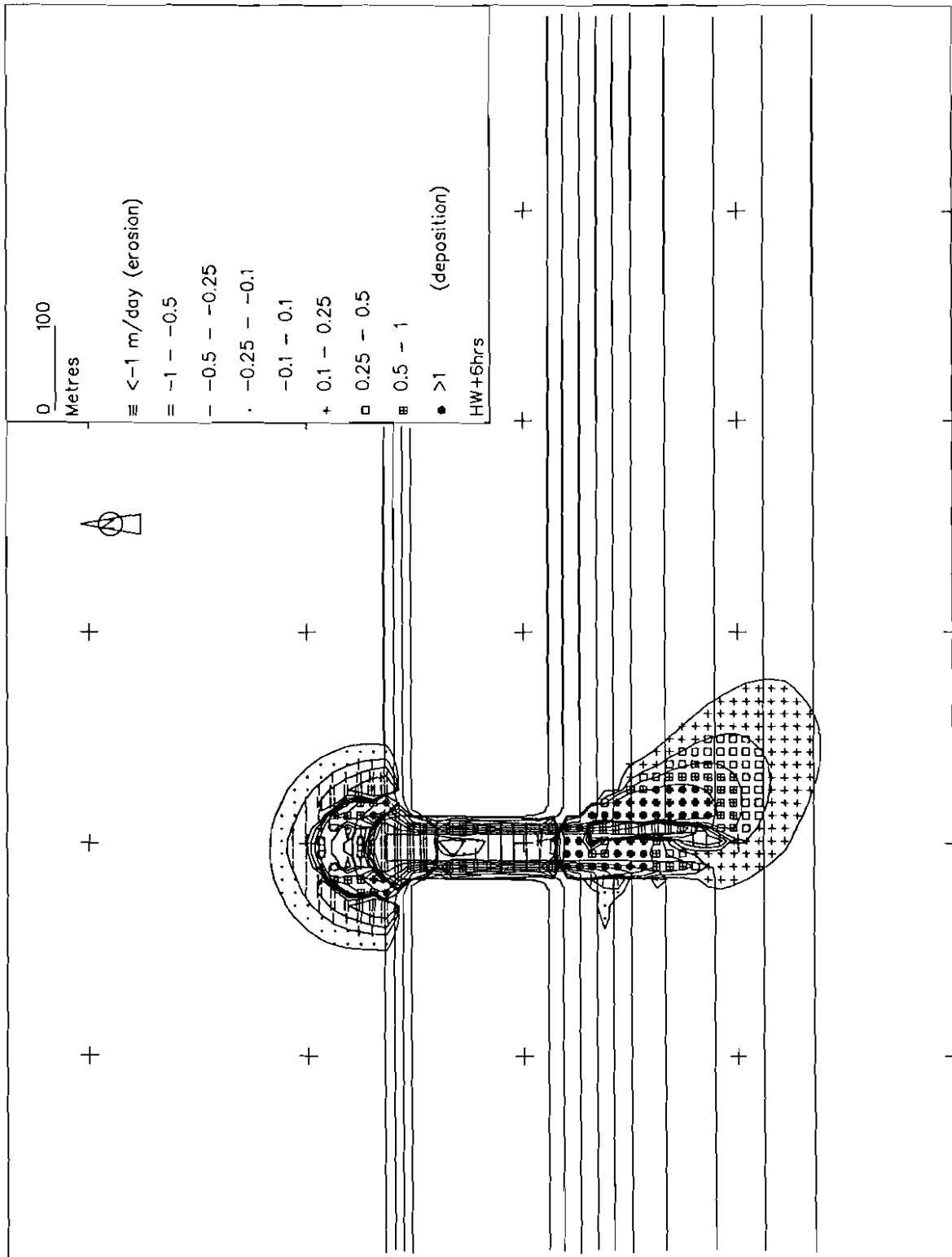


Figure 13 Silver Strand  
Tidal residual sand transport  
Vicinity of disposal mound  
Wave direction 77 N



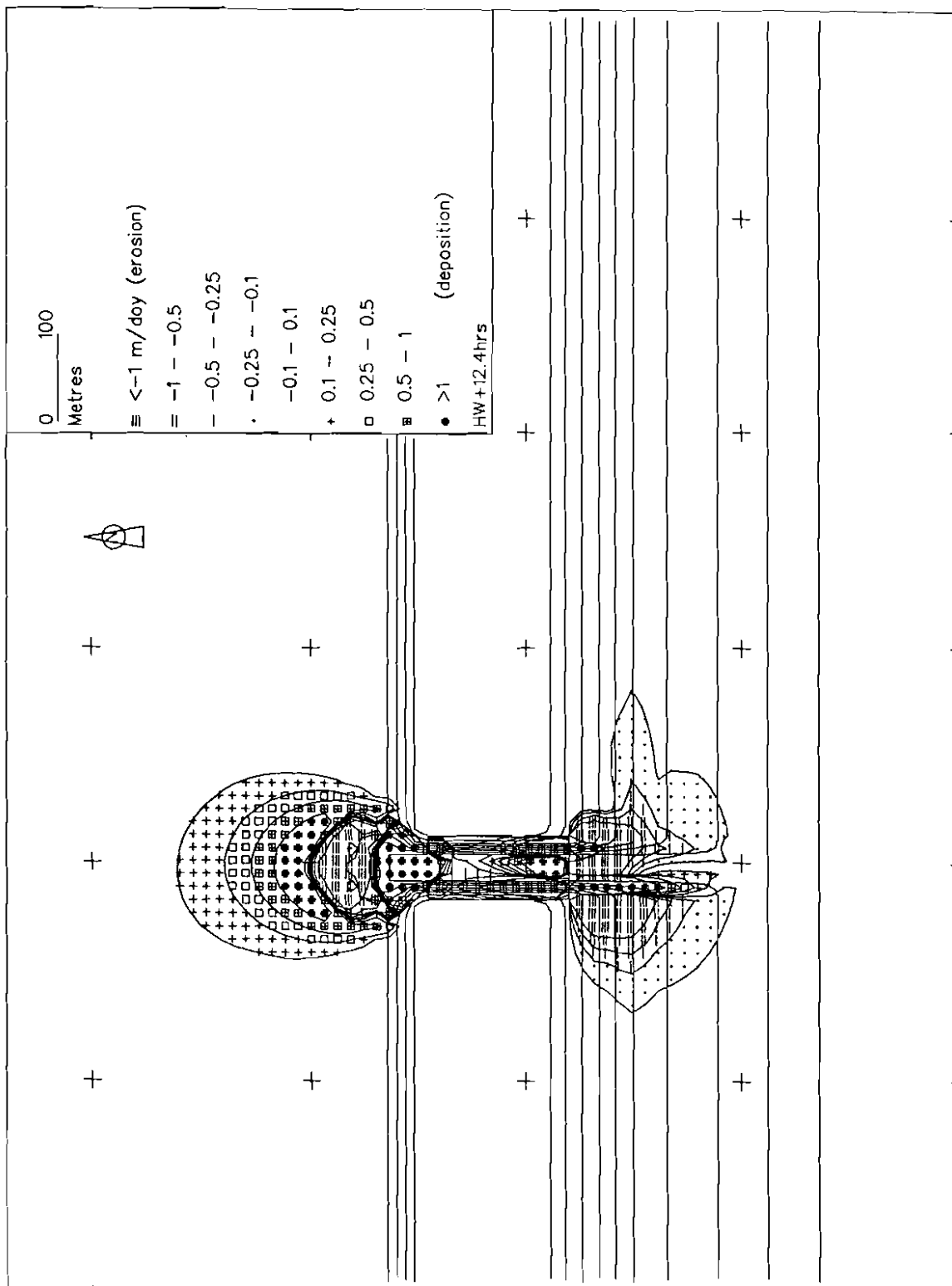
File Z created 18/06/93 at 14:00:51 plotted on 18/06/93 at 14:24

Figure 18 Keta Lagoon test case  
Velocity field  
HW + 12.4 hours



File keta\_FLUX created 18/06/93 at 14:01:13 plotted on 18/06/93 at 14:45

Figure 19 Keta Lagoon Study  
Rate of bed level change – static bed  
HW + 6 hours

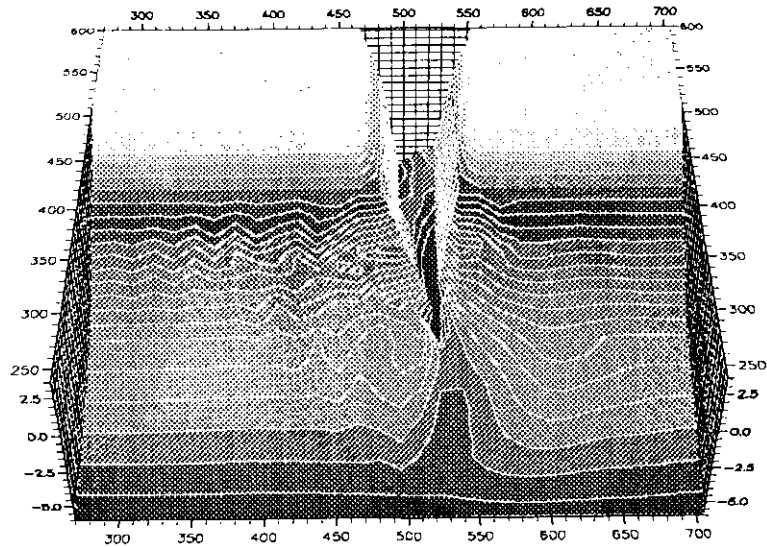


File ketc\_FLUX created 18/06/93 at 14:01:13 plotted on 18/06/93 at 14:46

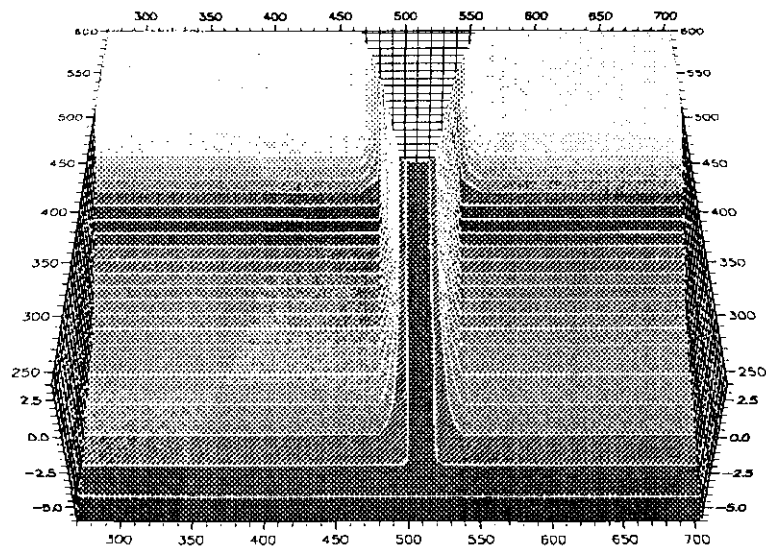
Figure 20 Keta Lagoon Study  
Rate of bed level change - static bed  
HW + 12.4 hours



## Updated bed after 9 tides



## Initial bathymetry



File Z created 13/01/95 at 12:32:11 plotted on 13/01/95 at 14:17

Figure 21 A) updated bed after 9 tides  
B) initial bathymetry

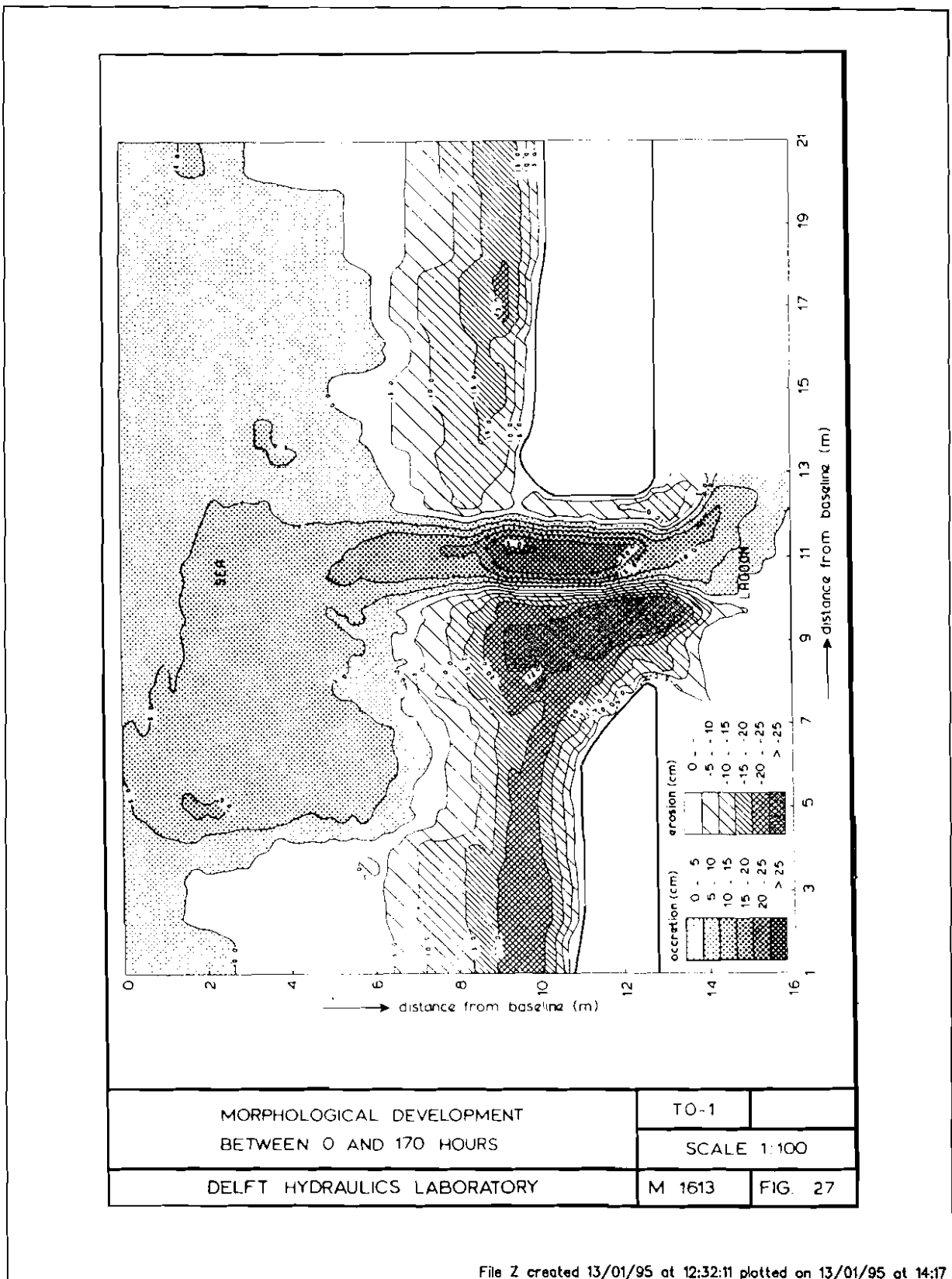
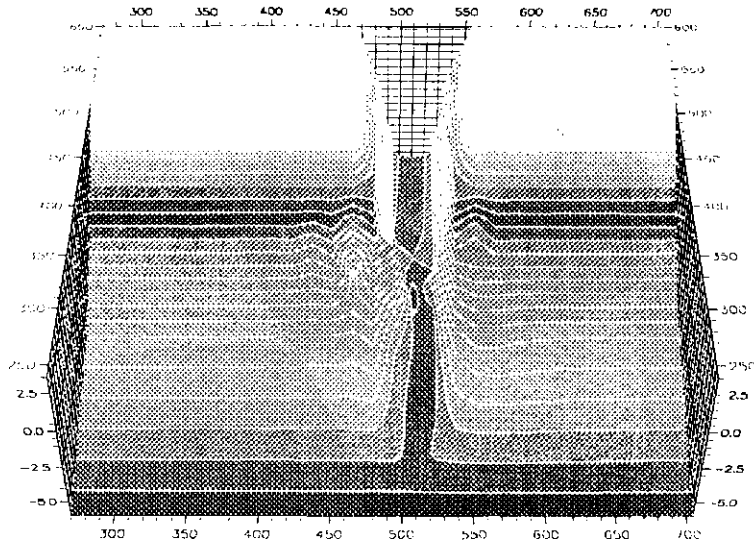


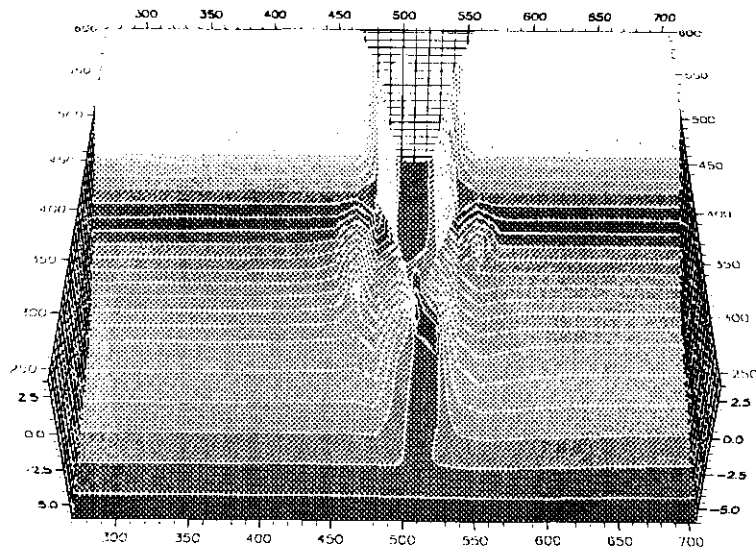
Figure 21 C) physical model bathymetry after 170 hours



After 1 tide, intertidal update



After 1 tide, tidal update



File Z created 13/01/95 at 12:32:11 plotted on 13/01/95 at 14:16

Figure 21 D) after 1 tide, intertidal update  
E) after 1 tide, tidal update

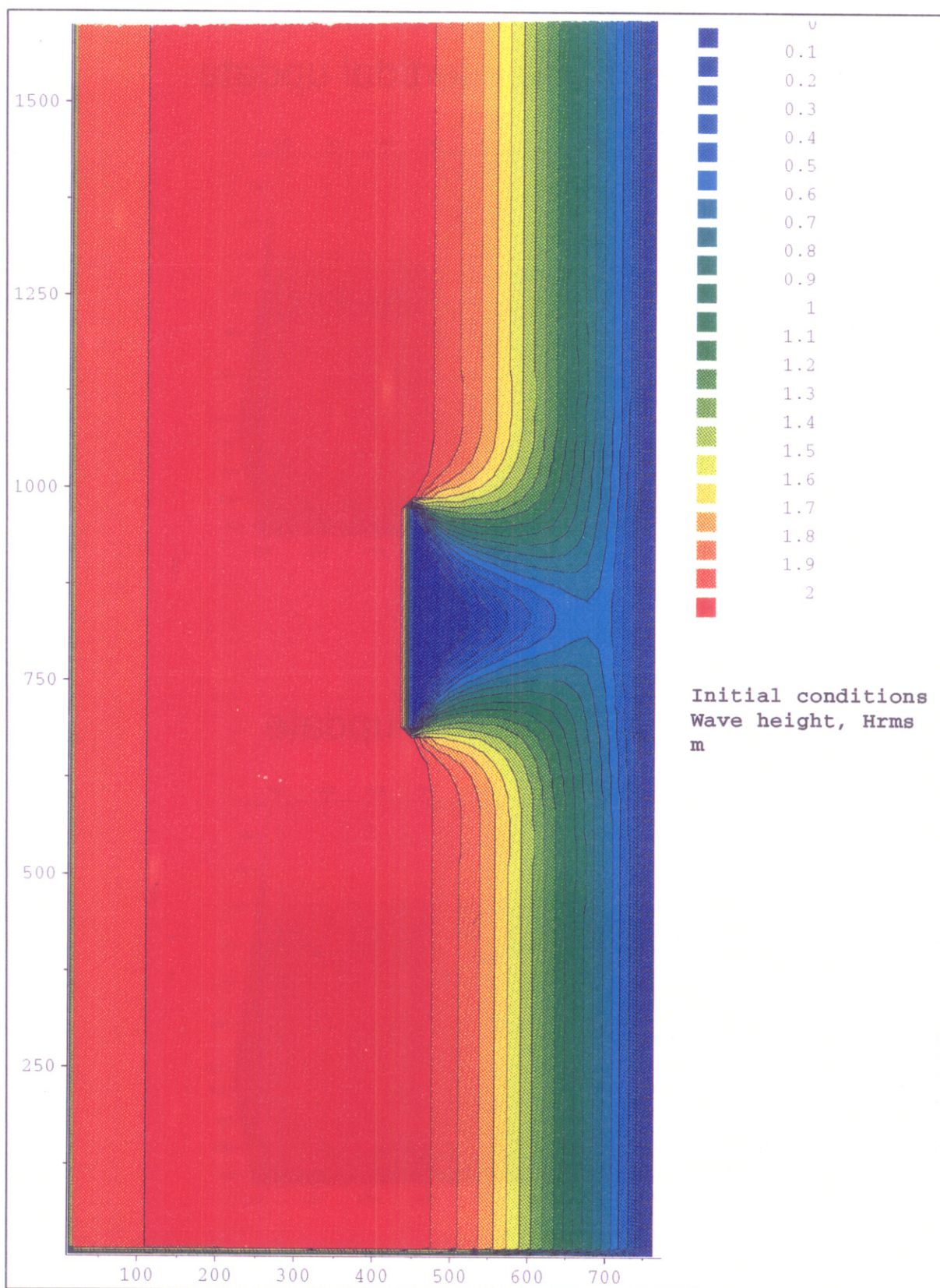


Figure 22 Detached breakwater, initial wave heights

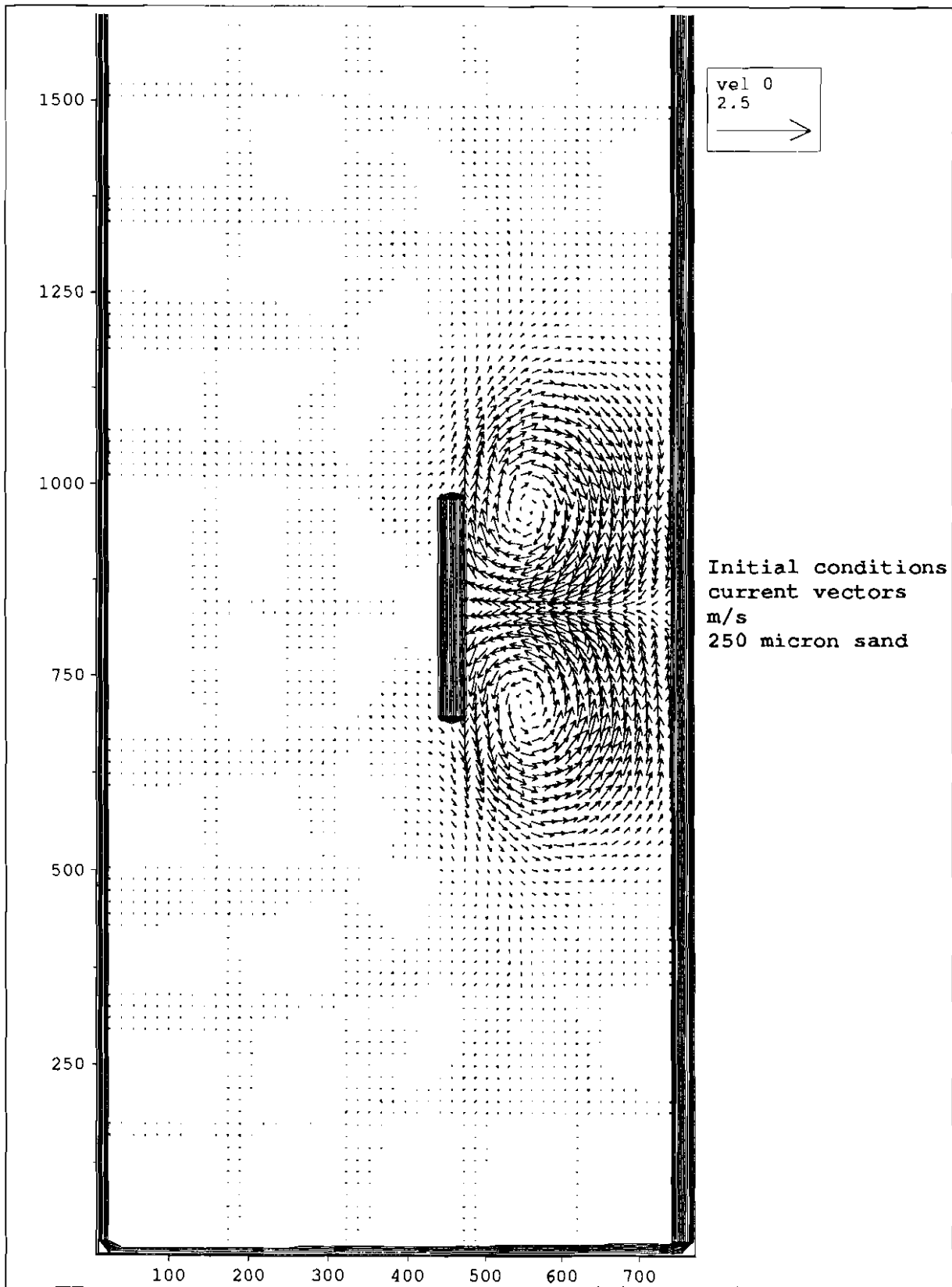


Figure 23 Detached breakwater, initial current field

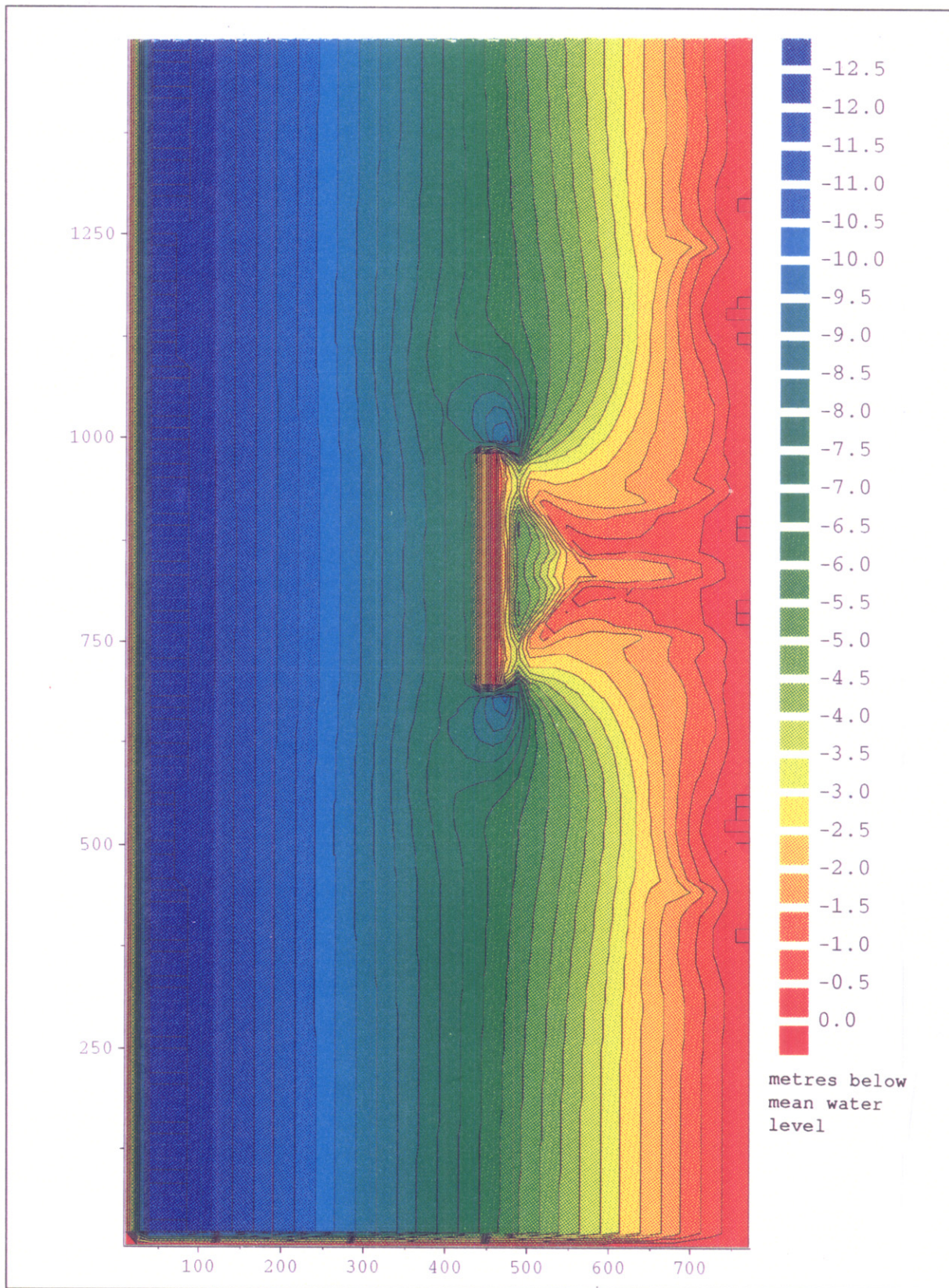


Figure 24 Detached breakwater,  
bed levels after 200 hours  
250 micron sand

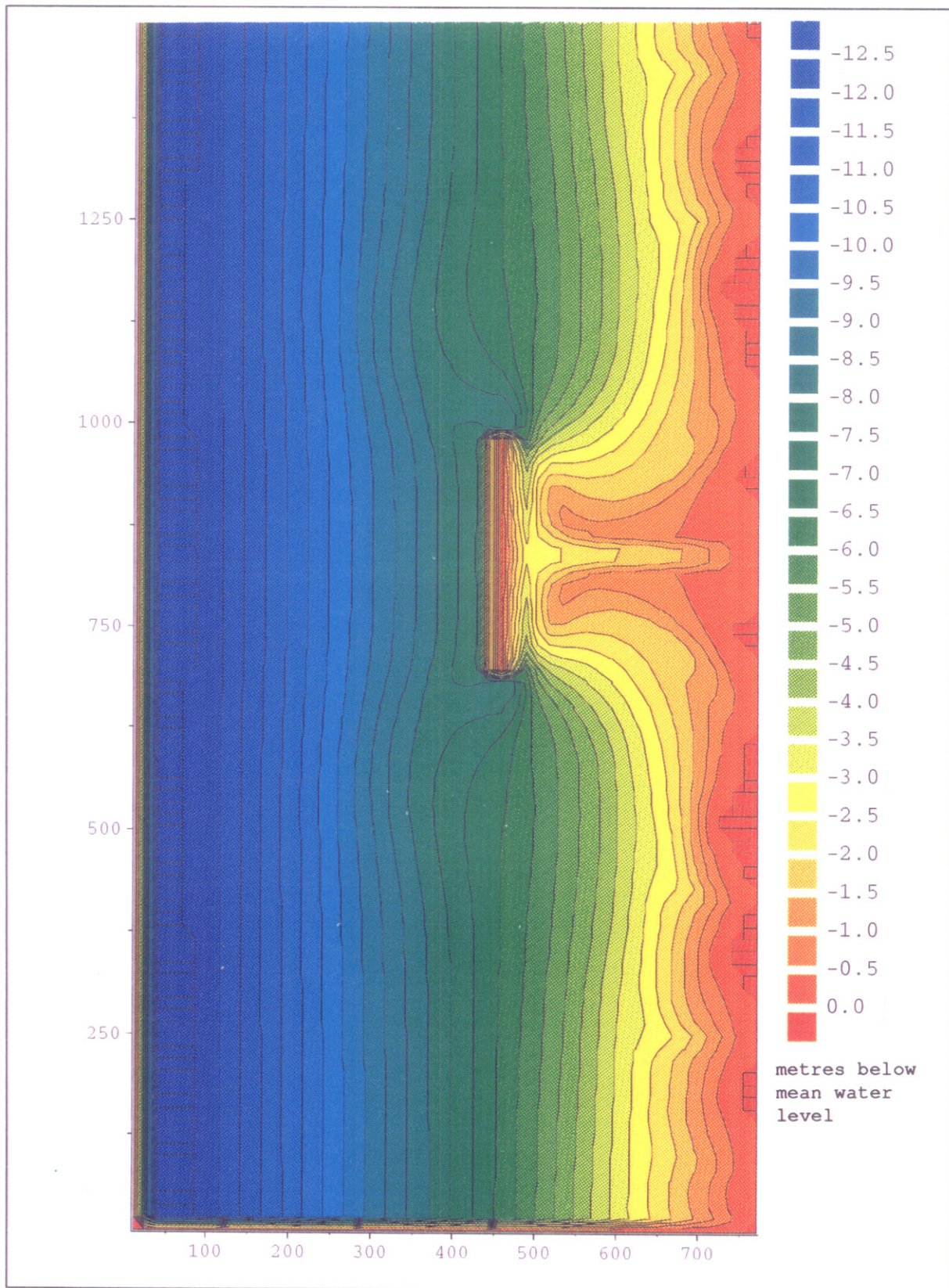


Figure 25 Detached breakwater,  
bed levels after 200 hours  
100 micron sand





## **Appendix**

Description of SANDFLOW-2D model





## **Appendix Description of SANDFLOW-2D Model**

### **Purpose**

Using the flows calculated by TIDEFLOW-2D to study the transport, deposition and erosion of non-cohesive (sandy) sediment and thereby identify areas of potential siltation and erosion.

### **Introduction**

The sediments under consideration here are very fine and fine sands ( $d_{50} \sim 0.06$  to  $0.25$  mm) which mainly move in suspension. The model can also be used to identify trends in the case of medium sand ( $d_{50} \sim 0.25$  to  $0.5$  mm). If the sediment contains a high proportion of clay or silt particle sizes less than  $0.06$  mm it would be more appropriate to use the MUDFLOW-2D model.

The main factors controlling sand transport are:

- advection by currents
- settlement under gravity
- turbulent diffusion in all directions (but only the vertical component is of significance under most circumstances)
- exchange of sediment between the flow and the bed

The study of sand transport generally is very difficult but more so in the case of estuaries or coastal areas because the water movements are continually changing with the rise and fall of the tide and there is usually a wide range of sediments on the bed and areas without mobile sediment leading to unsaturated loads in the water.

### **Method**

Although sand transport in estuaries is really an unsteady, 3D problem it has been shown by HR Wallingford that it can be dealt with using a 2D, depth-averaged model provided special provision is made to account for the vertical profile effects of the sediment concentration. Under these circumstances the depth-averaged, suspended solids concentration  $c(x, y, t)$  satisfies the conservation of mass equation.

$$\frac{\partial}{\partial t}(dc) + \alpha \left[ \frac{\partial}{\partial x}(duc) + \frac{\partial}{\partial y}(dvc) \right] = \frac{\partial}{\partial s}(dD_s \frac{\partial c}{\partial s}) + \frac{\partial}{\partial n}(dD_n \frac{\partial c}{\partial n}) + S \quad (1)$$

where

- (u,v) = depth-averaged components of velocity (m/s)
- $D_s$  = longitudinal (shear flow) dispersion coefficient ( $m^2/s$ )
- $D_n$  = lateral (turbulent) diffusivity ( $m^2/s$ )
- (x,y) = Cartesian co-ordinates in horizontal plane (m)
- (s,n) = are natural co-ordinates (parallel with and normal to mean flow) (m)
- t = time (sec)
- d = water depth (m)
- S = erosion from or deposition on the bed ( $kg/m^2/s$ )



$\alpha$  = advection factor to recover the true sediment flux from the product of depth-averaged quantities

Advection factor ( $\alpha$ )

This is introduced to compensate for the omission of the vertical profile in the sediment flux terms.

$$\alpha = T/qcd \quad (2)$$

where

$d$  = water depth (m)

$T$  =  $\int_0^d q'c'dz$  is the sand transport (kg/m width/s)

$q$  = the depth-averaged water speed  $(u^2 + v^2)^{1/2}$  and  $q',c'$  are the full three-dimensional velocity and concentration variables.

Since the highest concentrations occur near the bed it follows that  $\alpha \leq 1$ . Typical values of  $\alpha$  can be obtained by evaluating equation (2) for sand transport profile observations or from the integration of theoretical solutions for suspended solids profiles. However in practice it is usually acceptable to take  $\alpha = 1$  on the grounds that the external and internal

sources of mobile sediment are not well enough known to justify a more precise formulation.

### Bed exchange relations

The simplest formulation of the bed exchange relation is

$$S = \beta_s \omega_s (c_s - c) \quad (3)$$

where

$c_s$  is the depth-averaged concentration when the flow is saturated with sediment (kg/m<sup>3</sup>)

$\omega_s$  is the representative settling velocity (m/s) and

$\beta_s$  is a profile factor to compensate for integrating out the vertical profile of suspended sediment ie to correct for higher sediment concentrations near the bed.

Deposition or erosion takes place depending as to whether the instantaneous sediment load ( $c$ ) exceeds or is less than the saturated value ( $c_s$ ), and pick up of sediment from the bed is prevented if there is no sediment available on the bed. A shortage of material on the bed is reflected in a low concentration of suspended solids being advected away by the flow.

Typical values of  $\beta_s$  could be obtained from actual observations of sediment profiles or from theoretical considerations. However, HR Wallingford have derived an analytical expression for this so that bed exchanges are performed automatically. This involves simplifying the vertical diffusivity relation and a profile mixing factor is introduced to enable the user to increase or decrease the effective mixing during calibration of the model.



## Sediment transport relation

The evaluation of bed exchanges requires a depth-averaged sediment concentration ( $c_s$ ). Sandflow-2D obtains this from a sediment transport relation specified by the user. Two sand transport relations are supplied in the package ( van Rijn and a simple power law).

The choice of sand transport relation needs care. It should be borne in mind that most relationships found in the literature are based on river or channel data where sediments are more narrowly graded than in estuaries. Also there is normally a small proportion of cohesive material in estuary sediments and this can alter the transport properties. If possible, sand fluxes should be measured at the study site, and if such data is available it may be best to use it to obtain the best-fit power law relation for the site. Alternatively the user can select the van Rijn sediment transport relation option.

These formulae for currents only can be written in total load flux form as:

$$q_t = AU(U - U_{cr})^{n-1} \quad (8)$$

where A and n are constants dependent on the transport law used.

By appealing to the method of Grass, the effects of waves on the sediment transport, including a threshold velocity, is defined as suggested by Soulsby (private communication) by:

$$q_{t,w} = AU[(U^2 + BW^2)^{0.5} - U_{cr}]^{n-1} \quad (9)$$

where

- B = 0.08/C<sub>D</sub>
- W is the r.m.s. wave orbital velocity (m/s)
- C<sub>D</sub> is the drag coefficient

The effect of bed slope on the transport is represented according to Struiksma and Crosato (1989) by:

$$q_{t,g} = q_{t,w} \left[ 1 - \frac{\beta \partial h}{\partial s} \right] \quad (10)$$

where

- s is the streamwise coordinate
- $\beta$  is a constant of order 1
- h is the bed level relative to fixed model datum (m)

## Diffusion

The dispersion ( $D_s$ ) and diffusion ( $D_n$ ) coefficients are not well defined. When viewed in close enough detail the whole motion appears advective; but when viewed on a coarser grid the smallest motions appear diffusive. Thus selection of the appropriate diffusion or dispersion coefficients depends on the grid size of the model - one model will treat as advection what a coarser grid model will treat as diffusion or dispersion.

Fortunately, the solutions to the equation are not normally sensitive to  $D_s$  and  $D_n$ . As a first approximation,  $D_n = Bdu$ , where d and u are representative depths and velocities. It has been found that B is usually in the range 0.01



(for fairly uniform depths and smooth beds) to 0.1 (for irregular geometry and/or rougher beds).

$D_s$  is automatically calculated by the program for each model cell depending on the local depth and velocity to give more diffusion in the direction of flow. The overall scale of  $D_s$  can be changed using the relative dispersion parameter. This normally has the value unity but it can be adjusted upwards or downwards during calibration to get agreement between the model results and any dispersion observations which may be available.

### **Numerical method**

A simple, explicit, upstream finite difference technique is used to solve the advection - diffusion equation. Flux corrections are not considered to be necessary because the background concentrations of suspended sand are normally fairly uniform.

The use of an explicit method introduces a stability constraint on the computing timestep ( $\Delta t$ ).

$$\Delta t < \Delta s / (\text{maximum flow velocity})$$

Where  $\Delta s$  is the grid size (m):

This does not normally pose any problems in practice because the allowable  $\Delta t$  is usually much larger than the TIDEFLOW-2D timestep and there is only a single equation to solve in the process model compared to three in TIDEFLOW-2D. Under these circumstances an explicit method is preferred because it enables the user to understand the code more easily and modify the treatment of the physics of the processes being simulated.

The treatment of the dispersion ( $D_s$ ) and diffusion ( $D_n$ ) terms introduces another stability constraint.

$$\Delta t < \Delta s^2 / 4 D_{\max}$$

Where  $D_{\max}$  is the maximum of  $D_s$  and  $D_n$

This constraint is normally weaker than the advective stability limit but the user should be aware that a high value of diffusivity can lead to an instability so in the event of problems the possible violation of both limits should be checked.

### **Application of model**

The application of the model and interpretation of the results requires a good understanding of sand physics. Firstly it is important to choose representative values for the main parameters. Ideally these should be based on laboratory tests of actual sediment samples from the site. It is also important for the modeller to be aware of the limitations of this type of model when applied to real sites.

It is also important to appreciate that sand transport is not an exact science. Accordingly, whatever model is used, and whatever parameter values are



chosen it is essential that results are interpreted correctly. Provided this is done the model will be a valuable engineering tool.

### **Calibration/validation**

Calibration of sediment models is difficult because bed changes are usually too slow or too variable to measure anything significant for comparison. Sometimes historical charts or dredging records may be available but even then it is unlikely that the sources of suspended sediment can be quantified for the relevant period. Sometimes it is possible to get scaling factors for model results in cases where information is available and use these to estimate siltation in the new situation, but in many cases one is forced to use the best available values for the parameters and to demonstrate that the siltation and erosion patterns produced by the model agree with the observed state of the estuary or coastal region being studied.

Some evidence to support the physical realism of the model is given by the following results of simulation of sand transport in a flume and of observations from the Thames estuary.

The computer model results were compared with the results of a laboratory experiment performed in a flume with a length of 30m, a width of 0.5m and a depth of 0.7m. The discharge was measured by a circular weir. The mean flow depth was 0.25m and the mean flow velocity was 0.67 m/s. The bed material had a  $d_{50} = 230\mu\text{m}$  and a  $d_{90} = 320\mu\text{m}$ . The median diameter of the particles in suspension was estimated to be about  $200\mu\text{m}$ , resulting in a representative fall velocity of 0.22 m/s (water temperatures  $9^{\circ}\text{C}$ ). The stream bed was covered with bed forms having a length of about 0.1m and a height of about 0.015m. Small Pitot tubes were used to determine the vertical distribution of flow velocity. Water samples were collected simultaneously by means of a siphon method at four locations to determine the spatial distribution of the sand concentrations. At each location (profile) five samples were collected at a height of about 0.015, 0.025, 0.05 and 0.22m above the average bed level and these were integrated to give the suspended load transport. The HR SANDFLOW-2D model was run for the same conditions assuming the overall shear velocity was 0.0477 m/s and the results in Figure 1 shows that the model could be calibrated if suitable data is available.

The model was compared with some flume data to test its response to a change in the sediment load. It was shown that the model simulation could be calibrated by adjusting the settling velocity and vertical diffusivity parameters. This procedure is justified for practical applications because in nature these parameters are not well defined. For example, there is no unique settling velocity because the suspended load would contain a range of sediment sizes and the true nature of the vertical diffusivity is not yet fully understood.

The basic physics of the model was then checked against real field data from Foulness in the Thames Estuary. There was a wide range of sediment sizes in the data but the model was only used to simulate individual fractions. The saturation concentrations in the model were calculated using a cubic velocity relation derived from the observed sand fluxes.

Results from the model simulation of the 75 to  $100\mu\text{m}$  sand fraction are shown in Figures 2 and 3 plotted at half hourly intervals with a sequence



number showing the progression through the tide. The model has a similar hysteresis effect to the observations on both stages of the tide. The systematic underestimation of concentrations during the ebb is probably due to a different availability of sediment sizes not allowed for in the simplified model. Nevertheless the demonstration confirms the general validity of the model in a natural situation.

An example of the agreement achieved during validation, between the SANDFLOW-2D model results and observed sediment distribution is shown in Figure 4. Note in particular the agreement between the areas of potential erosion predicted by the model and areas of rock bed, and also the areas of potential deposition and areas of sand bed observed.

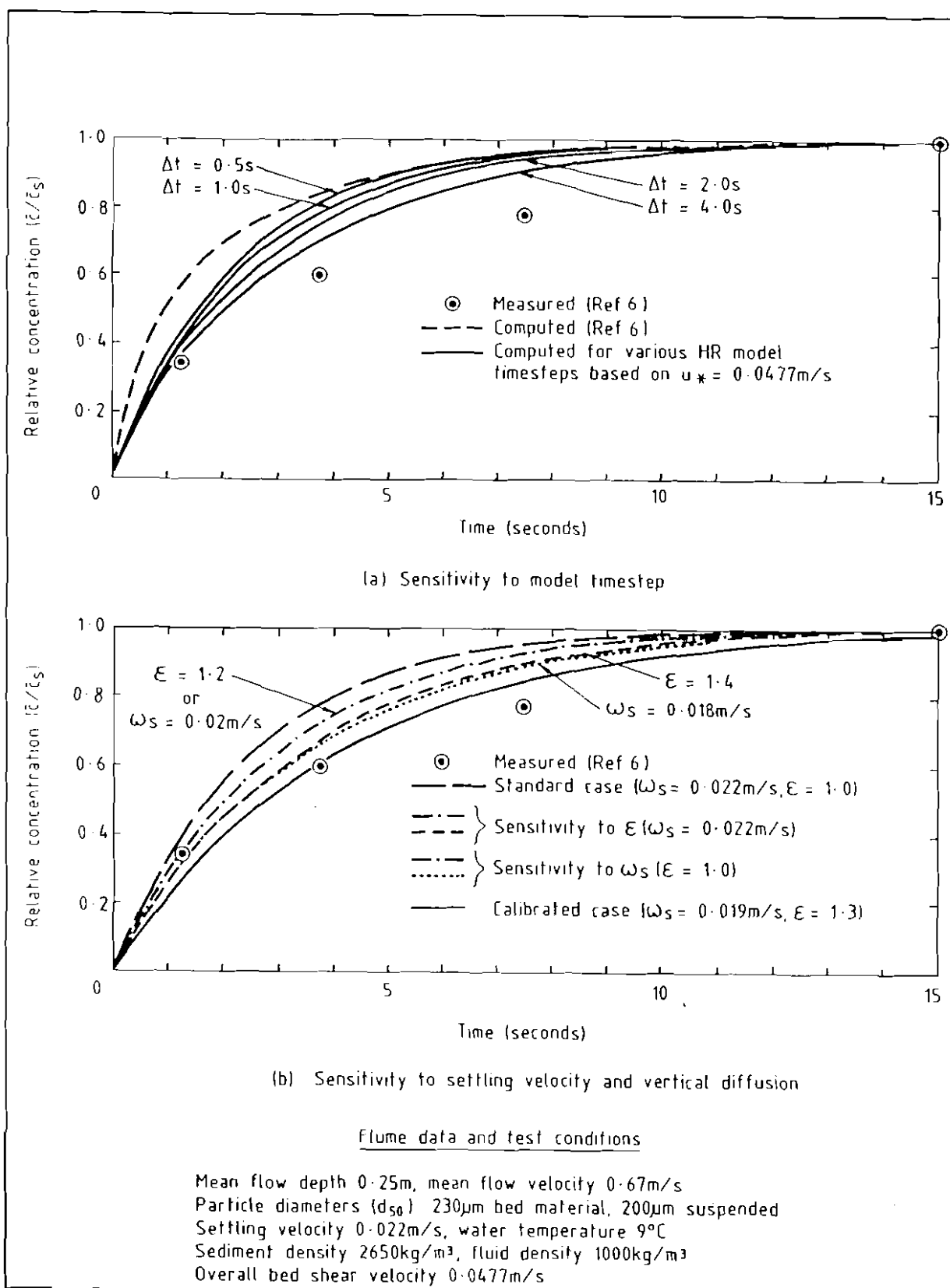


Figure A1 Computed and measured evolutions of sediment load

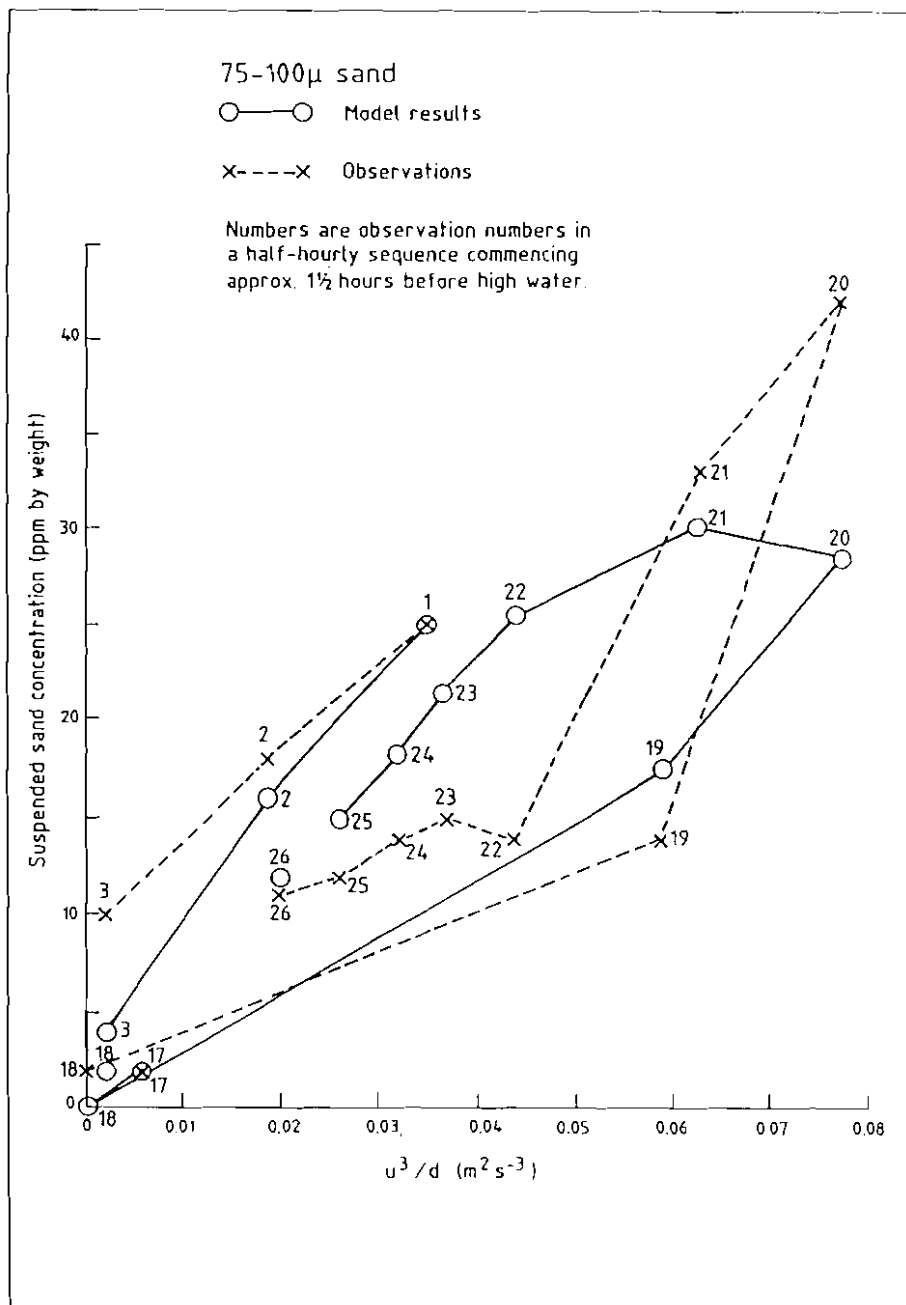


Figure A2 Simulation of Foulness position 1 flood tide

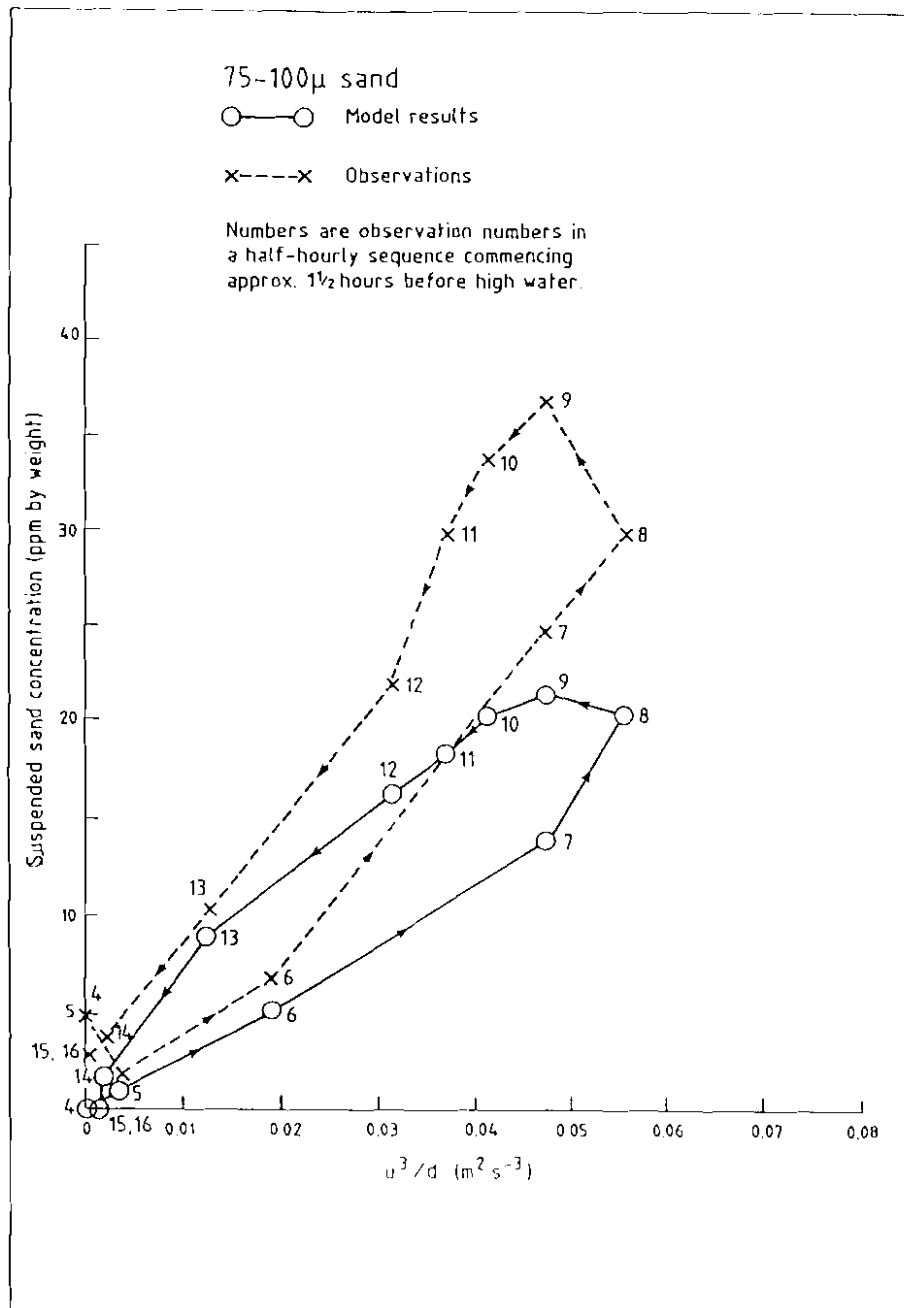


Figure A3 Simulation of Foulness position 1 ebb tide

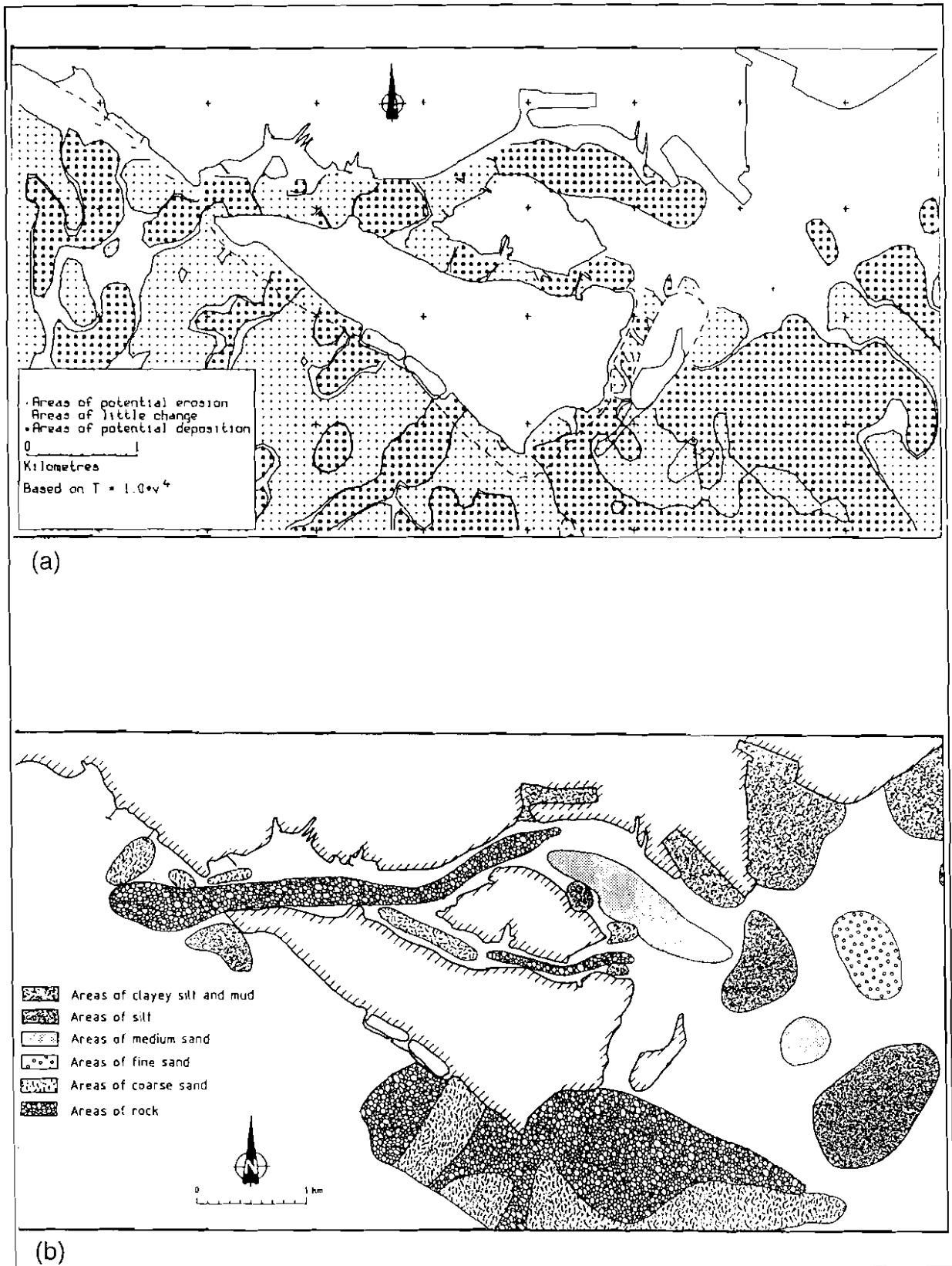


Figure A4 Comparison of sand erosion/deposition areas in model (a) with observed sediment distribution (b)